Title: Phylogenomic analyses provide insights into primate evolution

Authors: Yong Shao [1 *], Long Zhou [2 *], Fang Li [3, 4], Lan Zhao [5], Bao-Lin Zhang [1], Feng Shao [6], Jia-Wei Chen [7], Chun-Yan Chen [8], Xu-Peng Bi [2], Xiao-Lin Zhuang [1, 9], Hong-Liang Zhu [7], Jiang Hu [10], Zongyi Sun [10], Xin Li [10], Depeng Wang [10], Iker Rivas-González [11], Sheng Wang [1], Yun-Mei Wang [1], Wu Chen [12], Gang Li [13], Hui-Meng Lu [14], Yang Liu [13], Lukas Kuderna [15], Kyle Kai-How Farh [16], Peng-Fei Fan [17], Li Yu [18], Ming Li [19], Zhi-Jin Liu [20], George P Tiley [21], Anne D Yoder [21], Christian Roos [22], Takashi Hayakawa [23, 24], Tomas Marques-Bonet [15, 25], Jeffrey Rogers [26], Peter D Stenson [27], David N. Cooper [27], Mikkel Heide Schierup [11], Yong-Gang Yao [9, 28, 29, 30], Ya-Ping Zhang [1, 29, 30], Wen Wang[1, 8, 29], Xiao-Guang Qi [5, †], Guojie Zhang[1, 2, 3, 31, †], Dong-Dong Wu [1, 29, 30, 32, †]

Affiliations:

1. State Key Laboratory of Genetic Resources and Evolution, Kunming Natural History Museum of Zoology, Kunming Institute of Zoology, Chinese Academy of Sciences, Kunming, 650201, China.
2. Center of Evolutionary & Organismal Biology, and Women's Hospital at Zhejiang University School of Medicine, Hangzhou, 310058, China
3. Section for Ecology and Evolution, Department of Biology, University of Copenhagen, Copenhagen, DK-2100, Denmark
4. Institute of Animal Sex and Development, ZhejiangWanli University, Ningbo, China
5. Shaanxi Key Laboratory for Animal Conservation, College of Life Sciences, Northwest University, Xi'an, China
6. Key Laboratory of Freshwater Fish Reproduction and Development (Ministry of Education), Southwest University School of Life Sciences, Chongqing 400715, China
7. BGI-Shenzhen, Shenzhen 518083, China
8. School of Ecology and Environment, Northwestern Polytechnical University, Xi'an, 710072, China
9. Kunming College of Life Science, University of the Chinese Academy of Sciences, Kunming, 650204, China
10. Grandomics Biosciences, Beijing 102206, China
11. Bioinformatics Research Centre, Aarhus University, Aarhus C., DK-8000, Denmark
12. Guangzhou Zoo & Guangzhou Wildlife Research Center, Guangzhou, 510070, China
13. College of Life Sciences, Shaanxi Normal University, Xi'an, China
14. School of Life Sciences, Northwestern Polytechnical University, Xi'an, China
15. Institute of Evolutionary Biology (UPF-CSIC), PRBB, Dr. Aiguader 88, 08003 Barcelona, Spain
16. Illumina Artificial Intelligence Laboratory, Illumina Inc, San Diego, CA, USA
17. School of Life Sciences, Sun Yat-sen University, Guangzhou, Guangdong 510275, China
18. State Key Laboratory for Conservation and Utilization of Bio-Resource in Yunnan, School of Life Sciences, Yunnan University, Kunming, China
19. CAS Key Laboratory of Animal Ecology and Conservation Biology, Institute of Zoology, Chinese Academy of Sciences, Beijing 100101, China
20. College of Life Sciences, Capital Normal University, Beijing 100048, China

21. Department of Biology, Duke University, Durham, NC 27708, USA
22. Gene Bank of Primates and Primate Genetics Laboratory, German Primate Center, Leibniz Institute for Primate Research, Göttingen 37077, Germany
23. Faculty of Environmental Earth Science, Hokkaido University, Sapporo, Hokkaido 060-0810, Japan
24. Japan Monkey Centre, Inuyama, Aichi 484-0081, Japan
25. Institut de Biologia Evolutiva, Pompeu Fabra University and Spanish National Research Council, 08003 Barcelona, Spain
26. Human Genome Sequencing Center, Department of Molecular and Human Genetics, Baylor College of Medicine, Houston, TX 77030, USA
27. Institute of Medical Genetics, School of Medicine, Cardiff University, Cardiff, CF14 4XN, UK
28. Key Laboratory of Animal Models and Human Disease Mechanisms of Chinese Academy of Sciences & Yunnan Province, Kunming Institute of Zoology, Chinese Academy of Sciences, Kunming, Yunnan, 650201, China
29. Center for Excellence in Animal Evolution and Genetics, Chinese Academy of Sciences, Kunming, Yunnan 650223, China
30. National Resource Center for Non-Human Primates, Kunming Primate Research Center, and National Research Facility for Phenotypic & Genetic Analysis of Model Animals (Primate Facility), Kunming Institute of Zoology, Chinese Academy of Sciences, Kunming, Yunnan 650107, China
31. Liangzhu Laboratory, Zhejiang University Medical Center, 1369 West Wenyi Road, Hangzhou 311121, China
32. KIZ-CUHK Joint Laboratory of Bioresources and Molecular Research in Common Diseases, Kunming Institute of Zoology, Chinese Academy of Sciences, Kunming 650204, China

*These authors contributed equally to this work.
†Corresponding authors:
Dong-Dong Wu: wudongdong@mail.kiz.ac.cn;
Guojie Zhang: guojiezhang@zju.edu.cn;
Xiao-Guang Qi: qixg@nwu.edu.cn.

Abstract

Comparative analysis of primate genomes within a phylogenetic context is essential for understanding the evolution of human genetic architecture and primate diversity. We present such a study of 50 primate species spanning 38 genera and 14 families, including 27 genomes first reported here, with many from previously less well represented groups, the New World monkeys and the Strepsirrhini. Our analyses reveal heterogeneous rates of genomic rearrangement and gene evolution across primate lineages. Thousands of genes under positive selection in different lineages play roles in the nervous, skeletal and digestive systems and may have contributed to primate innovations and adaptations. Our study reveals that many key genomic innovations occurred in the Simiiformes ancestral node and may have had an impact on the adaptive radiation of the Simiiformes and human evolution.

One-Sentence Summary: Comparative genomics reconstructs the evolutionary processes within the primates.

Main text

The order Primates contains more than 500 species from 79 genera and 16 families (*1*), with new primate species continuing to be discovered (*2-5*), making primates the third most speciose order of living mammals after bats (Chiroptera) and rodents (Rodentia). As our closest living relatives, non-human primates play important roles in the cultures and religions of human societies (*1*). Many non-human primate species have been widely used as animal models, on the basis of their genetic, physiological and anatomical similarities to humans, to allow the efficacy and safety of newly developed drugs and vaccines to be tested (*6*). For example, since the emergence of COVID19, macaques have served as important models in the research and development of vaccines (*7-16*). Primates display considerable morphological, behavioural and physiological diversity, and hold the key to understanding the evolution of our own species, particularly the evolution of human phenotypes such as high level cognition (*17*, *18*).

Non-human primates occupy a wide range of diverse habitats in the tropical forests, savanna, semi-desert and subtropical regions of Asia, Central and South America, and Africa, whilst humans have spread across much of the earth's surface. Nevertheless, according to the International Union for Conservation of Nature (IUCN) Red Lists, more than a third of primate species are critically endangered or vulnerable, about 60% of primate species are threatened with extinction, while 75% of primate species are experiencing population decline (*1*). With global climate change and increasing anthropogenic interference, the conservation status of primates has attracted global scientific and public awareness.

Despite their importance, reference genomes have been sequenced in fewer than 10% of non-human primate species (*19-27*), a state of affairs that both impedes research and hampers conservation efforts. Here we present high quality reference genomes for 27 primate species with long read sequencing generated from our first phase program of the Primate Genome Project.

Assembly and annotation of 27 new primate reference genomes

We applied long-read genome sequencing technologies, including Pacbio and Nanopore, to sequence the genomes of 27 non-human primate species from 26 genera of 11 families (table S1). Long reads were self-polished and assembled, and the genome assemblies were further corrected and polished by paired-end short reads sequenced from the same individuals (tables S2-S4). We also used sequencing data generated by high-throughput Chromosome Conformation Capture technology (*28*) to anchor assembled contigs into chromosomes for four species (Fig. S1 and table S4). The sizes of the newly assembled genomes of the primate species under study ranged from ~2.4 Gbp (*Daubentonia madagascariensis*) to ~3.1 Gbp (*Erythrocebus patas*), which were mostly consistent with the k-mer–based estimations (Fig. S2 and table S5), with a high average contig N50 length of ~15.9 Mbp (table S6). All the genome assemblies yielded BUSCO complete scores >92% (table S6). A method that integrates *de novo* and homology-based strategies was applied to annotate all genomes with protein sequences from human, chimpanzee, gorilla, orangutan and mouse as references for homology-based gene model prediction. Totals of between 20,066 and 21,468 protein-coding genes were predicted in these genome assemblies (table S7). Further, we also identified ~24.2 Mb primate-specific highly conserved elements by using whole-genome alignments between all primates and nine other mammals (Fig. S3).

The Primate Genome Project also generated high quality reference genomes for another 16 primate species which were used in the other accompanying papers to reveal hybrid speciation during the rapid radiation of the macaques (*29*), the homoploid hybrid speciation in the snub-nosed monkey *Rhinopithecus* genus (*30*), social evolution in the Asian colobines driven by cold adaptation (*31*), and the evolutionary adaptations of slow lorises (*32*). All genomic data have been published openly and can be freely accessed in the NCBI Assembly Database under the accession information described in this study.

A genomic phylogeny of living primates

We next performed phylogenomic analyses comprising the 27 newly generated genomes, another 22 published primate genomes, one long-read genome from *Nycticebus pygmaeus* reported in an accompanying paper (*32*), and two close relatives of primates, the Sunda flying lemur (*Galeopterus variegatus*) and the Chinese tree shrew (*Tupaia belangeri chinensis*) (*33*), as outgroups (table S8). We constructed whole genome-wide phylogenetic trees using ExaML under a GTR+GAMMA model (*34*). Altogether, ~ 433.5 Mbp gap-free data of syntenic orthologous sequences were retrieved from the whole-genome alignments (table S9), and were used to infer the primate phylogeny, yielding a high-resolution whole-genome nucleotide evidence tree with identical topology to a previous tree derived from 54 nuclear gene regions from 186 living primates (*35*). This tree has 100% bootstrap support for all evolutionary nodes, with the exception of the node [((*Symphalangus syndactylus*, *Hoolock leuconedys*), *Hylobates pileatus*)] among gibbon genera with 90% bootstrap support (Figs. 1, S4 and S5). The evolution of gibbons has been characterized by their rapid karyotypic changes, and remains controversial in primate phylogeny at the genus level (*24, 35, 36*). To confirm the phylogeny of this node, we also generated partitioned trees with orthologous protein-coding genes, exon codons with 1st and 2nd positions, four-fold degenerate sites and

conserved non-exonic elements (Figs. S6-S9). The tree from conserved non-exonic elements yielded the identical topologies for the gibbon lineages with the whole-genome nucleotide evidence trees (Fig.S9). However, the trees from orthologous protein-coding genes/exon codons with 1st and 2nd positions and four-fold degenerate sites respectively supported the alternative topologies, [((*Nomascus*, *Hylobates*), (*Symphalangus*, *Hoolock*))] and [((*Nomascus*, (*Symphalangus*, *Hoolock*)), *Hylobates*)] (Figs. S6-S8). The two topologies were shown in previous studies based on variants called by mapping short-reads to the reference genome of *Nomascus leucogenys (24, 36)*.

Our analyses again confirmed the phylogenetic challenge within the gibbon lineage which has experienced pronounced adaptive radiation within an extremely short evolutionary time period (*24, 35*). Consistently, we observed extremely short internal branches in this lineage on the phylogeny. A comparative analysis using CoalHMM (*37*) across primate lineages showed that the gibbon lineage represents one of the lineages with the highest frequency of incomplete lineage sorting (*38*), supporting a previous study based on population data (*24*). Specifically, the two gibbon branches showed incomplete lineage sorting proportions of 57% and 61%, respectively, but the species topology inferred from incomplete lineage sorting analyses is identical to those presented in this paper (Figs. S4 and S10).

Based on the whole-genome nucleotide evidence tree and fossil calibration data (*35, 39*) (Figs. 1 and S11), the divergence dating of living primates was estimated by means of the MCMCtree algorithm (*40*) (Figs. 1 and S12). We estimated that the most recent common ancestor of all primates evolved between 64.95 and 68.29 million years ago (Mya), which is close to the estimate given in the latest phylogenetic study across mammals (*41*), suggesting the origin of the primate group near the Cretaceous/Tertiary boundary at 65Mya. Meanwhile, we also estimated that the most recent common ancestor of Strepsirrhini appeared between 52.57 to 56.56 Mya and that of the Simiiformes emerged between 35.65 to 42.55 Mya (Figs. 1 and S12).

Genomic structure and evolution of primates

Karyotype evolution and genome rearrangement

The speciation process is often accompanied by karyotypic evolution, which would also impact genome evolution and gene function (*42-44*). We reconstructed the ancestral karyotype evolutionary process across primate lineages (table S10) and observed an overall conserved pattern of chromosome-level synteny (Fig. 2A). The numbers of ancestral karyotypes of Catarrhini (2*n*=46) and Hominoidea (2*n*=48) were consistent with previous inferences derived from the fluorescence in situ hybridization data of bacterial artificial chromosomes (*45*) (Fig. 2A). However, we deduced that both of the ancestral karyotypes of primates and Simiiformes had a diploid number of 2*n*=52 (Fig. 2A), rather than 2*n*=50 as previously suggested (*45*), recovering a fission event in Chromosome 8 which was observed in the common ancestor of primates (Figs. 2A and S13). Fusion and fission are the most common mechanisms of karyotype evolution in primates, as exemplified by the fusion of Chromosome 2 which occurred specifically in the human lineage (*45*). Our analyses further identified at least one fission and one fusion during the emergence of the Simiiformes, as well

as one fission and four fusions associated with the Catarrhini node (Figs. 2B and S13), resulting in the contemporary karyotype structure of our own. The rapid change of karyotypes in the Simiiformes also led to an increased chromosome number in New World monkeys which possess the largest number of chromosomes across primates. We further estimated the rate of genome rearrangement by taking account of all large-scale genomic rearrangement events including reversions, translocations, fusions and fissions in key evolutionary nodes from the primate common ancestral lineage leading to the human lineage. We observed an increasing rate of rearrangement in the Homininae (*Gorilla-Homo-Pan*) (~2.38/Mya) and particularly in the Hominini (*Homo-Pan*) (~5.56/Mya) (Fig. 2B), which contradicts the Hominini slowdown hypothesis on the nucleotide substitution rates (*35*).

Lineage-specific segmental duplication

We next compiled segmental duplication maps (Segmental duplication length ≥ 5kbp) for primates and 5 outgroup species (Fig. S14 and table S11). Compared with other primate lineages, we observed a striking increase in the number of lineage-specific segmental duplications (221 specific segmental duplications) in the great ape genomes (Fig. 3A and table S12), consistent with previous findings describing a burst of segmental duplications in the great ape ancestor (*46*). These specific segmental duplications in great apes overlapped with 57 protein-coding genes (table S13), 20 of which were highly expressed in the human brain (Fig. S15). Additionally, we also observed lineage-specific segmental duplications in other primate groups producing lineage-specific novel genes that might have contributed to the evolution of these lineages (table S13). We further explored the functions of all genes overlapping segmental duplications in primate genomes (table S13) against the Human Gene Mutation Database (*47*) and found that a high proportion of these genes (52.8%) have been reported to be associated with inherited conditions including autism, intellectual disability and other developmental disorders (Fig. 3B and table S14).

Evolution of genome size and transposable elements

Compared to other mammalian groups, the primates have a relatively large genome size on average (*48*, *49*). Among primates, the lemurs (Lemuriformes + Chiromyiformes) were found to be characterized by a significantly smaller genome size (~2.36 Gbp) than those of other groups, such as the lorisoids (Lorisiformes: Lorisdae + Galagidae) (~2.70 Gbp), New World monkeys (~2.82 Gbp), Old World monkeys (~2.91 Gbp) and Hominoidea (~2.96 Gbp) ($P < 0.05$, Mann-Whitney U test) (Fig. S16). The increase of genome size in the Simiiformes can be attributed to the expansion of transposable elements (Figs. S16-S18 and table S15), especially *Alu* elements, ~300 nucleotide short interspersed sequence elements (SINEs) that make up ~11% of the human genome (*50-54*). We observed that the genomes of lemurs exhibited a relative paucity of SINEs, especially *Alu* (~3.87%), which is less than one third of the proportion noted in other lineages (Figs. S16-S18). By contrast, the *Alu* elements in both Simiiformes and Lorisiformes experienced major bursts of retrotranspositional activity at ~40-45 and ~34-39 Mya independently (Fig. S19). Specifically, we noticed a dramatic expansion of the *AluS*-related subclasses especially *AluSx* in the Simiiformes, whilst the *AluJ*-related subclasses (especially *AluJb*) were the dominant subclasses of *Alu* in the Lorisiformes (Fig. S20).

Variation in the nucleotide substitution rate

We estimated the overall nucleotide substitution rate in primates to be around 1.1×10^{-3} substitutions per site per million years (Figs. 3C, S21, and table S16), which is much lower than the average rate for mammals (~2.7×10^{-3} substitutions per site per million years) and birds (~1.9×10^{-3} substitutions per site per million years) (*55*). However, the nucleotide substitution rate exhibited a high degree of heterogeneity between primate lineages, potentially due to differences with respect to life history traits (*56-58*). The New World monkeys evolved the fastest at ~1.4×10^{-3} substitutions per site per million years (Figs. 3C and S21). We confirmed the hominoid 'slowdown' (*35, 59-61*) hypothesis by detecting a reduced substitution rate in hominoids (~0.8×10^{-3} substitutions per site per million years) (Fig. S21). Meanwhile, our analysis and a previous study (*62*) suggest that tarsiers, as the most basal haplorrhines, potentially evolved with a rapid substitution rate compared to other primates (Fig. S21).

Evolution of protein-coding genes

We obtained a high-confidence orthologous gene set comprising 10,185 orthologs across 50 primate species, Sunda flying lemur and Chinese tree shrew. Based on the whole-genome nucleotide evidence tree topology of primates, we calculated d_N/d_S [the ratio of the rates of nonsynonymous (d_N) to synonymous (d_S) substitutions] for each ortholog to explore the evolutionary constraints operating on coding regions. Based upon the observation that tissue-specific expressed genes are generally conserved across diverse species (*63, 64*), we estimated the evolutionary rate of tissue-specific expressed genes for different tissues across evolutionary clades in primates, and observed that testis- and spleen-specific expressed genes generally display higher values of d_N/d_S (Figs. 3D, S22, and S23) than other tissue-specific expressed genes, corroborating the rapid evolution of the reproductive and immune systems in primates (*65, 66*). By contrast, brain-specific expressed genes generally showed a high degree of conservation with lower d_N/d_S values as previously reported, despite the rapid evolution of primate cognitive functions (*67*).

Next, we detected 82 positively selected genes in the common ancestral lineage of primates by comparison with other mammalian species (table S17) using the codeml algorithm under the branch-site model with a likelihood rate test in PAML4 (*40, 68*). We found that these positively selected genes were significantly enriched in genes exhibiting high level expression in brain, bone marrow and testis (table S18). In particular, close to 37% (30 genes) of positively selected genes exhibited biased expression in the brain (tables S18 and S19), and we found that some of them, e.g., *SPTAN1*, *MYT1L* and *SHMT1*, should have important roles in brain function, because deleterious mutations of these genes have been reported to cause brain disorders (*69-71*) such as 'epilepsy' and 'schizophrenia'. These genes may be important candidates for involvement in the evolution of the primate brain because of their functional importance. Our results suggest that some positively selected genes in the primate ancestral lineage may have been involved in the rapid evolution of their brain functions, despite the general conservation of brain-specific expressed genes. In addition, several immune-related genes (e.g., *XRCC6* and *CD2*) (table S17) also experienced positive selection in the primate

ancestor, suggesting that the adaptive immune system might also have contributed to primate evolution.

An increased level of genomic change in the ancestor of the Simiiformes

To provide new insights into the genetic underpinnings of primate phenotypic evolution, we performed various comparative genomic analyses including identification of positively selected genes, genes having conserved non-coding regions that have been subject to lineage-specific accelerated evolution (*72*), and expanded gene families in different primate lineages (*68*). Intriguingly, an increased level of genomic evolutionary changes, reflected by the high numbers of positively selected genes, lineage-specific accelerated regions and expanded gene families, was observed in the Simiiformes ancestor (Fig. 4A). Consistently, the Simiiformes have also experienced rapid evolution of a series of complex traits in contrast to the Strepsirrhini and Tarsiiformes. For example, the Simiiformes generally exhibit a larger brain volume and body mass than the Strepsirrhini and Tarsiiformes (Fig. 4B) (*73, 74*). Functional enrichment analyses showed that the associated genes relevant to these rapid genomic changes in the Simiiformes ancestor (tables S20-S22) were over-represented in functions related to the nervous system and development, such as postsynaptic density, synapse and the negative regulation of the canonical Wnt signaling pathway (table S23).

Additional analyses indicated that various candidate genes in the Simiiformes ancestral lineage, comprising 168 positively selected genes, 273 genes associated with lineage-specific accelerated regions, and 14 expanded gene families, were enriched in central nervous system terms, i.e., brain, cerebrum, cerebellum, hippocampus and cerebral cortex (table S24). More specifically, five genes participated in the pathway ‘axon guidance’ (Fig. 4C), being expressed in the human brain at a high level (table S25). Axon guidance represents a key stage in the formation of a neural network (*75, 76*) and may have been an important influence on brain volume. In this pathway, two semaphorin genes (*SEMA3B* and *SEMA3D*), which are critical for central nervous system patterning (*77, 78*), experienced positive selection and served as a gene associated with the lineage-specific accelerated region, respectively. These two genes, together with another three genes associated with the lineage-specific accelerated regions (*EPHA3*, *RAC1* and *NTNG2*), are known to be important for brain development (*79-81*). Furthermore, eight genes were assigned under the term ‘Hippo signaling pathway’ (Fig. 4D), an evolutionarily conserved signaling pathway, which controls organ or body size by regulating cell growth, proliferation and apoptosis in a range of animals, from flies to humans (*82-84*). Taken together, genes involved in neuronal network formation and the control of organ size appear to have undergone adaptive evolution in the Simiiformes ancestral lineage and may have been responsible for specific phenotypic changes, particularly the progressive increase in brain volumes and body sizes as compared with the Tarsiiformes and Strepsirrhini.

A major phenotypic difference between the Strepsirrhini/Tarsiiformes and the Simiiformes is nocturnal versus diurnal life history. The visual system has diverged substantially between the Simiiformes and Strepsirrhini/Tarsiiformes such that the diurnal Simiiformes have much smaller corneal sizes (relative to their eyes) and higher visual acuity than the Strepsirrhini/Tarsiiformes (*85*). Consistent with this phenotypic difference, we detected

positive selection signals in three genes (*NPHP4*, *GRHL2* and *SLC39A5*) associated with 'eye development' (GO: 0001654) in the Simiiformes ancestral lineage. An intragenic deletion in *NPHP4* causes recessive cone-rod dystrophy with a predominant loss of cone function in the dachshund (*86*). *GRHL2* encodes a transcription factor that suppresses epithelial-to-mesenchymal transition; ectopic *GRHL2* expression due to mutation accelerates cell state transition and leads to posterior polymorphous corneal dystrophy and vision function disruption (*87*). The *GRHL2* gene has the highest number of positively selected sites in the Simiiformes ancestor compared with the other genes involved in 'eye development' (Fig. S24). *TAS1R1* encodes a taste receptor which can form a heterodimer with TAS1R3 to elicit the umami taste (*88*). We found that *TAS1R1* also experienced positive selection with four positively selected sites in the Simiiformes ancestor (Fig. 4E). The rapid and concerted evolution of taste receptors and vision could have helped the diurnal Simiiformes to locate and identify food. The detailed functional consequences of these amino acid changes might be worthy of further study.

Compared to the Strepsirrhini/Tarsiiformes, the Simiiformes generally exhibit darker skin pigmentation and a less bright coat colour (Fig. S25) (*89*). We identified two pigmentation-related genes (*KIT* and *CREB3L4*) participating in the 'Melanogenesis' pathway that evolved under positive selection (detected by the branch-site model) in the Simiiformes ancestor (Fig. 4E). Melanocytes play an important role during the formation of skin and coat colors in mammals by regulating melanin-related genes (*90*). *KIT,* a proto-oncogene, encodes a receptor tyrosine kinase which regulates cell migration, proliferation and differentiation in melanocytes and plays a key role in melanin deposition (*91, 92*). Additionally, *KIT* also communicates with *MITF*, a key gene in the formation of melanin which regulates the development of melanocytes (*93-95*).

Genetic mechanisms underlying primate phenotype evolution

Primates have evolved diverse phenotypic traits in order to adapt to their challenging environments. Here, we sought to investigate the evolution of complex phenotypes in the brain, skeletal system, body size, digestive system and sense organs in primates.

Brain evolution

In primates, brain volumes range from less than about 2 cm^3 in the mouse lemur to approximately 1300 cm^3 in human (*73*). To reveal the genetic changes that might underlie brain evolution in primates, we detected signals of positive selection in brain development genes using a branch-site model in PAML in key evolutionary nodes in the primate phylogeny. A total of 34 brain genes were found to be under positive selection in one of the primate evolutionary nodes (table S26) (*68*). Four of them (*SLC6A4*, *NR2E1, NIPBL,* and *XRCC6*) were under positive selection in the common ancestor of all primates whereas 30 were under positive selection in other primate ancestral nodes leading to the evolution of human (table S26). These results appear to suggest that primates underwent continuous brain evolution over an extended period of evolutionary time. Knockout experiments on many of these positively selected genes have shown brain function impairment in mice. For instance, the *NIPBL* gene interacts with *ZFP609* to regulate the migration of cortical neurons, and its

mutations are frequently involved in brain neurological defects encompassing intellectual disability and seizures (*96*). We identified two amino acid residues in the NIPBL protein which experienced adaptive change in the common ancestor of all primates lineage (Fig. S26).

Microcephaly is characterized by severe neurological defects, the small brain size being caused by disturbance of the proliferation of nerve cells (*97*). Some genes involved in microcephaly have been proposed as candidates for involvement in the evolution of brain size (*98-100*). We also searched for positive selection signals in the 1,113 coding genes involved in Microcephaly (HP:0000252). In total, 65 positively selected genes with functional roles in microcephaly were identified along with the primate ancestor leading to the human lineage (table S27), suggesting that microcephaly genes may have been involved in the dramatic evolutionary expansion of brain size that characterizes primates, especially in those crucial evolutionary nodes characterized by a sharp increase in the degree of cortical folding (gyrification) and brain volume (*101*).

We next sought to investigate the roles of regulatory elements in the evolution of primate brain size. We first identified non-coding regions that were highly conserved and under strong purifying selection across all primates, and detected signals of accelerated evolution in four lineages [the Simiiformes ancestor (table S21), the Catarrhini ancestor (table S28), the ancestor of great apes (table S29), and the human lineage (table S30)], representing crucial evolutionary nodes for the enlargement of primate brain size (*101*) (Fig. S27). These lineage-specific accelerated regions should be under strong positive selection specifically in the targeted lineages and might contribute to the adaptation or innovation of these lineages (*72*). We found 15 genes associated with lineage-specific accelerated regions in the common ancestor of the great apes which showed particularly high expression in the human fetal brain (Fig. S27 and table S31) ($P = 0.023$, Modified Fisher's Exact test); over half of these genes have been reported to have roles in brain development and function (*102-109*). For example, knockout of the transcription factor-encoding *MEF2C* in a mouse model results in impaired neuronal differentiation and smaller somal size among neural progenitor cells (*108*). Coincidentally, the lineage-specific accelerated region of this gene was detected in the great ape ancestral lineage. The *DLG5* gene, required for polarization of citron kinase in mitotic neural precursors, also contains a lineage-specific accelerated region in the great ape lineage, and *DLG5*$^{-/-}$ mice have smaller brains and thinner neocortices (*109, 110*).

We further investigated the evolution of neurotransmitters, which mediate the neurogenesis process in brain (*111*, *112*) and also play a role in the regulation of brain size (*111*). We detected 12 positively selected genes and 39 genes associated with lineage-specific accelerated regions in the ancestral nodes leading to the human lineage that were found to be involved in the release, transportation and reception of neurotransmitter signals (Figs. 5A and S28); these genes participate in diverse neurotransmitter systems (i.e., glutamatergic, dopaminergic, cholinergic and GABAergic synapses, and the synaptic vesicle cycle). Among these genes, 5 positively selected genes and 33 genes associated with lineage-specific accelerated regions are highly expressed in human brain (table S32). Taken together, it is

likely that at least some of these genomic changes impacting the neurotransmitter signaling pathway might have played a role in primate brain evolution.

Evolution of the skeletal system and limbs

The arboreal lifestyle co-evolved with adaptive changes of the skeletal system and limb development. Here, genes functioning in bone development are likely to have been especially important for the adaptive radiation of the primates. We identified four positively selected genes (*PIEZ01*, *EGFR*, *BMPER* and *NOTCH2*) that were involved in bone development (*113-116*) in the ancestral lineage of primates (table S17). Bone development requires the recruitment of osteoclast precursors from the surrounding mesenchyme, thereby actuating the key events of bone growth such as marrow cavity formation, capillary invasion and matrix remodelling. Mechanical sensing protein PIEZO1 accommodates bone homeostasis via osteoclast-osteoblast crosstalk (*113*). Osteoclasts then influence osteoblast formation and differentiation through the secretion of some soluble factors (*117*). In the meantime, *EGFR* negatively regulates mTOR signaling during osteoblast differentiation to control bone development (*114*). The *NOTCH2* gene regulates cancellous bone volume and microarchitecture in osteoblast precursors (*116, 118*).

Although tails vary across the primates in terms of their length and shape, they generally play key roles in relation to locomotion (*119*). This notwithstanding, the tail was secondarily lost in some primate lineages including the common ancestor of the apes (*120, 121*). We retrieved 151 genes associated with lineage-specific accelerated regions in the common ancestral lineage of the apes (table S33), including *KIAA1217* (sickle tail protein homolog) (Figs. S29 and S30). Mutations in *KIAA1217* are associated with malformations of the notochord and caudal vertebrae in human and affect the development of the vertebral column leading to a characteristic short tail due to a reduced number of caudal vertebrae in mouse (*122, 123*). Thus, the lineage-specific accelerated region may serve as a regulator of the expression of *KIAA1217* because this lineage-specific accelerated region, residing in the vicinity of *KIAA1217* in the ape lineage, overlaps with an enhancer EH38E1455433 (pELS) (Fig. S31). The high-throughput chromosome conformation capture data (Fig. S32) also showed that this lineage-specific accelerated region is located in the same topologically associated domain as *KIAA1217*, suggesting that they may physically interact with each other (Fig. S32). Furthermore, the lesser apes (gibbons) are of particular interest owing to their dominant locomotor style – brachiation (*124, 125*). This locomotor adaptation was accompanied by the acquisition of distinct morphological characteristics, particularly the elongated forelimb, representing one of the most intriguing phenotypic traits in gibbons, enabling them to travel through the canopy at high speed (*126*). We found that positive selection has operated on four genes related to upper limb bone morphology in the gibbon ancestral lineage (table S34). Of these, *NEK1*, which encodes a serine/threonine kinase, contains the most positively selected sites (Fig. 5B). Functional studies have shown that genetic variants in this gene can influence bone length and shorten the humerus and femur in humans (*127, 128*). Therefore, positive selection acting on genes related to upper limb bone morphology may have been important in the acquisition of the elongated forelimb, a key adaptive trait for the unique brachiating locomotion style of gibbons.

Evolution of body size in primates

Like other mammalian groups (*129, 130*), extant primate species exhibit a large body size range, from dwarf galagos and mouse lemurs (~60-70g) at one end of the spectrum to male gorillas (>200kg in some individuals) at the other (*131*). Thus, primate body size has experienced significant divergence, particularly for the great apes with their dramatic enlargement in body size. We detected several positively selected genes in the common ancestors of the great apes which might have contributed to the evolution of this trait. *DUOX2* encodes a protein involved in a critical step of thyroid hormone synthesis and mutations in *DUOX2* are known to cause decreased body size in mouse and panda (*132, 133*). This gene experienced strong positive selection in the great ape ancestral lineage (χ^2 test, $P = 0.018$) (Fig. 5C and table S35). Additionally, we noted several genes involved in the TGF-beta signaling pathway (e.g., *LTBP1*) or the Wnt signaling pathway (e.g., *MBD2*, *YAP1* and *DISC1*), two of the best known pathways participating in bone development and body size (*48*), that were either under strong positive selection in the great apes or which have lineage-specific accelerated regions in this lineage (Fig. 5C and tables S29 and S35).

Several positively selected genes and genes associated with lineage-specific accelerated regions in the great ape ancestor were also significantly overrepresented in the Hippo signaling pathway (P=0.045, Modified Fisher's Exact test) (table S36), which has been implicated in the determination of organ and body size (*82*). Interestingly, when combining all positively selected genes, genes associated with lineage-specific accelerated regions, and expanded gene families in the Simiiformes ancestral lineage, which dramatically increased their body size compared with non-Simiiformes lineages (Fig. 4B), we also detected diverse candidate genes with adaptive changes in the Hippo signaling pathway. These results indicate potentially important roles for the Hippo pathway in body size changes in these two nodes during primate evolution.

Evolution of the digestive system

Primate lineages have evolved diverse dietary habits and specialized digestive functions (*134*). In particular, leaf-eating Colobines, an African and Asian subfamily (Colobinae) of Old World monkeys, have evolved a uniquely specialized and compartmentalized foregut, with discrete alkaline and acidic sections (to cope with their folivorous diet), in which microbial fermentation can take place (*135, 136*). Although colobines eat leaves, fruits, flowers and seeds, they typically focus much of their feeding time on leaves [estimated range: ~34-81% of their annual diet] (*135*). Accordingly, these leaf-eaters are well adapted in terms of meeting their energy metabolism requirements, balancing micronutrients and protein intake, while also dealing with the toxins contained in their food plants (*137*).

In the ancestor of the Colobinae, we identified a number of pivotal digestive genes that underwent positive selection (table S37). Acyl-CoA dehydrogenase, encoded by the *ACADM* gene, is an important lipolytic enzyme which catalyzes the initial step in each cycle of mitochondrial fatty acid β-oxidation and plays a key role in metabolizing fatty acids derived from ingested foods (*138*). Energy-rich short-chain volatile fatty acids are produced by the

microbial fermentation process; these are absorbed by the host and make an important contribution to the energy budget of colobines (*135*). Therefore, rapid evolution of this gene, with two positively selected sites (V75M and A138C), may have been important for the absorption of fatty acids by Colobines (Fig. 5D and S33). *NOX1*, which is highly expressed in the colon, was identified as being under positive selection in the ancestor of the Colobinae (Fig. 5D and tables S37 and S38). *NOX1*-dependent ROS production can further regulate microorganism homeostasis in the ileum of mice (*139*). The rumens of ruminants and the saccus stomachs of Colobines, have developed a similar adaptive strategy to allow the microbial fermentation of high fibre foods, and hence are an example of convergent evolution. We found that *MYBPC1*, which has been shown to contribute to morphological and functional differences in the bovine rumen (*140*), also underwent positive selection in the ancestor of the Colobinae (Fig. 5D and table S37). In addition, 100 genes associated with lineage-specific accelerated regions were identified in the ancestral lineage of the Colobinae (table S39). Several of these genes were also highly expressed in the stomach, colon, pancreas and small intestine (Fig. 5D and table S38). Of these, *RNASE4* encodes a vital digestive enzyme, pancreatic ribonuclease 4, and is a paralog of *RNASE1* which is known to have undergone adaptive evolution by gene duplication in leaf-eating Colobines and howler monkeys (*26, 141*). Colobines may therefore have acquired adaptations to allow them to digest fatty acids and ribonucleic acids, whilst their unique foregut and intestinal microbiota enabled them to cope with their folivorous diet.

Evolution of sensory organs

In many mammals, olfaction is the dominant sense and provides much of the sensory information upon which animals rely to navigate, forage and avoid predators, or for social behaviour and courtship (*134*). Most Strepsirrhini species are nocturnal, whereas most Simiiformes are diurnal with well-developed colour vision systems attuned to their priorities in diurnal activity (*142-145*). By contrast, olfactory sensitivity would appear to have decreased in the Simiiformes as compared to the Strepsirrhini (*134, 146, 147*). Consistent with these findings, we found that the copy number of several specific olfactory receptor gene families was significantly reduced in the Simiiformes. For example, the olfactory receptor gene family, *OR52A*, underwent the significant contraction in the Simiiformes (40 species) with only ~0.7 copies on average, in contrast to ~3.4 average copies in the Strepsirrhini (nine species) (Figs. S34 and S35) (P = 4.072e-05, Mann-Whitney U test). Anatomically, Strepsirrhini are characterized by the presence of a rhinarium, a moist and naked surface around the tip of the nose which is present in most mammals including dogs and cats, but the rhinarium has been lost in the Simiiformes (*134, 147*). Olfactory bulb volume, which correlates with olfactory receptor neuron population size, is also larger in the Strepsirrhini than in the Simiiformes (*146, 148*). Intriguingly, the *LHX2* gene, which participates in olfactory bulb development (*149, 150*), experienced positive selection in the ancestor of the Strepsirrhini (P = 0.03, χ^2 test, table S40).

Demographic history of non-human primates

The IUCN lists more than a third of primates as being critically endangered or vulnerable (*1*). To evaluate the effects of climate change and human activity on their recent population

declines, we inferred their demographic histories over the past million years by using the pairwise sequentially Markovian coalescent model (PSMC) (*151*) for each primate species in this study (Fig. S36 and tables S16 and S41). Our data showed that most non-human primate species have experienced rapid population declines during the late Pleistocene (Figs. 6A and S37), consistent with the record of large mammal mass extinction in this period (*48, 152*). Although we did not observe a significant difference between endangered species and other species in terms of nucleotide diversity (Fig. S38 and table S42), we did detect a significant positive correlation between the median effective population size (*N*e) over the past ~20,000 years and nucleotide diversity ($P = 0.002$, Pearson's product-moment correlation, after phylogenetic correction) (Fig. 6B and table S42), indicating a long-term effect of *Ne* decline on the loss of genetic diversity. According to the historical demographic patterns, we further clustered all non-human primate species with similar trends of historical *N*e and found that 20 species have experienced a continual *N*e decline over the last 3 million years (My) (Fig. 6C). Of note, 65% of these species are now listed as being endangered or critically endangered (Figs. 6C and S39). This ratio is twice that of the remaining species suggesting that the prehistoric environmental effects (e.g., habitat fragmentation) (*26*) may also have driven population decline and contributed to the current endangered status of these species well before human interference in the modern era.

Conclusions

Understanding the evolution and genetic basis of human-specific traits requires a systematic comparison of genomes along the primate lineages. Previous studies of primate genomes have focused on genomic changes in the human lineage that influenced human brain functions and other traits (*120, 153-155*). Our comparative phylogenomic analyses across primate lineages have revealed some of the accumulated genomic changes at different primate ancestral nodes that may have contributed to the evolution of uniquely human traits. Of particular interest, we report a hitherto unreported increase in the rate of genomic change in the Simiiformes common ancestor that may have played a role in the later diversification of Simiiformes and the evolution of humans. Our comparative genomic analyses also yielded insights into the genetic basis of phenotypic diversity across primate lineages. With the rich diversity of morphology and physiology among non-human primates, further genomic analyses covering all primate species promise to provide an indispensable resource for comparative studies allowing expansion of the scope of biomedical research programs using primates as model systems. Further, increased knowledge of the genomic makeup and variations of non-human primates should help to identify risk factors for genetic disorders and enhance wildlife health management in both wild and captive members of these species.

References and Notes

1. A. Estrada, P. A. Garber, A. B. Rylands, C. Roos, E. Fernandez-Duque, A. Di Fiore, K. A. Nekaris, V. Nijman, E. W. Heymann, J. E. Lambert, F. Rovero, C. Barelli, J. M. Setchell, T. R. Gillespie, R. A. Mittermeier, L. V. Arregoitia, M. de Guinea, S. Gouveia, R. Dobrovolski, S. Shanee, N. Shanee, S. A. Boyle, A. Fuentes, K. C. MacKinnon, K. R. Amato, A. L. Meyer, S. Wich, R. W. Sussman, R. Pan, I. Kone, B.

Li, Impending extinction crisis of the world's primates: why primates matter. *Sci Adv* **3**, e1600946 (2017).

2. C. Roos, K. M. Helgen, R. P. Miguez, N. M. L. Thant, N. Lwin, A. K. Lin, A. Lin, K. M. Yi, P. Soe, Z. M. Hein, M. N. N. Myint, T. Ahmed, D. Chetry, M. Urh, E. G. Veatch, N. Duncan, P. Kamminga, M. A. H. Chua, L. Yao, C. Matauschek, D. Meyer, Z. J. Liu, M. Li, T. Nadler, P. F. Fan, L. K. Quyet, M. Hofreiter, D. Zinner, F. Momberg, Mitogenomic phylogeny of the Asian colobine genus *Trachypithecus* with special focus on *Trachypithecus phayrei* (Blyth, 1847) and description of a new species. *Zool Res* **41**, 656-669 (2020).
3. A. Nater, M. P. Mattle-Greminger, A. Nurcahyo, M. G. Nowak, M. de Manuel, T. Desai, C. Groves, M. Pybus, T. B. Sonay, C. Roos, A. R. Lameira, S. A. Wich, J. Askew, M. Davila-Ross, G. Fredriksson, G. de Valles, F. Casals, J. Prado-Martinez, B. Goossens, E. J. Verschoor, K. S. Warren, I. Singleton, D. A. Marques, J. Pamungkas, D. Perwitasari-Farajallah, P. Rianti, A. Tuuga, I. G. Gut, M. Gut, P. Orozco-terWengel, C. P. van Schaik, J. Bertranpetit, M. Anisimova, A. Scally, T. Marques-Bonet, E. Meijaard, M. Krützen, Morphometric, behavioral, and genomic evidence for a new orangutan species. *Curr Biol* **27**, 3487-3498 (2017).
4. P. F. Fan, K. He, X. Chen, A. Ortiz, B. Zhang, C. Zhao, Y. Q. Li, H. B. Zhang, C. Kimock, W. Z. Wang, C. Groves, S. T. Turvey, C. Roos, K. M. Helgen, X. L. Jiang, Description of a new species of *Hoolock* gibbon (Primates: Hylobatidae) based on integrative taxonomy. *Am J Primatol* **79**, e22631 (2017).
5. C. Li, C. Zhao, P. F. Fan, White-cheeked macaque (*Macaca leucogenys*): a new macaque species from Medog, southeastern Tibet. *Am J Primatol* **77**, 753-766 (2015).
6. J. Rogers, R. A. Gibbs, Comparative primate genomics: emerging patterns of genome content and dynamics. *Nat Rev Genet* **15**, 347-359 (2014).
7. B. Rockx, T. Kuiken, S. Herfst, T. Bestebroer, M. M. Lamers, B. B. Oude Munnink, D. de Meulder, G. van Amerongen, J. van den Brand, N. M. A. Okba, D. Schipper, P. van Run, L. Leijten, R. Sikkema, E. Verschoor, B. Verstrepen, W. Bogers, J. Langermans, C. Drosten, M. Fentener van Vlissingen, R. Fouchier, R. de Swart, M. Koopmans, B. L. Haagmans, Comparative pathogenesis of COVID-19, MERS, and SARS in a nonhuman primate model. *Science* **368**, 1012-1015 (2020).
8. A. Chandrashekar, J. Liu, A. J. Martinot, K. McMahan, N. B. Mercado, L. Peter, L. H. Tostanoski, J. Yu, Z. Maliga, M. Nekorchuk, K. Busman-Sahay, M. Terry, L. M. Wrijil, S. Ducat, D. R. Martinez, C. Atyeo, S. Fischinger, J. S. Burke, M. D. Slein, L. Pessaint, A. Van Ry, J. Greenhouse, T. Taylor, K. Blade, A. Cook, B. Finneyfrock, R. Brown, E. Teow, J. Velasco, R. Zahn, F. Wegmann, P. Abbink, E. A. Bondzie, G. Dagotto, M. S. Gebre, X. He, C. Jacob-Dolan, N. Kordana, Z. Li, M. A. Lifton, S. H. Mahrokhian, L. F. Maxfield, R. Nityanandam, J. P. Nkolola, A. G. Schmidt, A. D. Miller, R. S. Baric, G. Alter, P. K. Sorger, J. D. Estes, H. Andersen, M. G. Lewis, D. H. Barouch, SARS-CoV-2 infection protects against rechallenge in rhesus macaques. *Science* **369**, 812-817 (2020).
9. Q. Gao, L. Bao, H. Mao, L. Wang, K. Xu, M. Yang, Y. Li, L. Zhu, N. Wang, Z. Lv, H. Gao, X. Ge, B. Kan, Y. Hu, J. Liu, F. Cai, D. Jiang, Y. Yin, C. Qin, J. Li, X. Gong, X. Lou, W. Shi, D. Wu, H. Zhang, L. Zhu, W. Deng, Y. Li, J. Lu, C. Li, X. Wang, W.

Yin, Y. Zhang, C. Qin, Development of an inactivated vaccine candidate for SARS-CoV-2. *Science* **369**, 77-81 (2020).

10. J. Yu, L. H. Tostanoski, L. Peter, N. B. Mercado, K. McMahan, S. H. Mahrokhian, J. P. Nkolola, J. Liu, Z. Li, A. Chandrashekar, D. R. Martinez, C. Loos, C. Atyeo, S. Fischinger, J. S. Burke, M. D. Slein, Y. Chen, A. Zuiani, F. J. N. Lelis, M. Travers, S. Habibi, L. Pessaint, A. Van Ry, K. Blade, R. Brown, A. Cook, B. Finneyfrock, A. Dodson, E. Teow, J. Velasco, R. Zahn, F. Wegmann, E. A. Bondzie, G. Dagotto, M. S. Gebre, X. He, C. Jacob-Dolan, M. Kirilova, N. Kordana, Z. Lin, L. F. Maxfield, F. Nampanya, R. Nityanandam, J. D. Ventura, H. Wan, Y. Cai, B. Chen, A. G. Schmidt, D. R. Wesemann, R. S. Baric, G. Alter, H. Andersen, M. G. Lewis, D. H. Barouch, DNA vaccine protection against SARS-CoV-2 in rhesus macaques. *Science* **369**, 806-811 (2020).

11. V. J. Munster, F. Feldmann, B. N. Williamson, N. van Doremalen, L. Pérez-Pérez, J. Schulz, K. Meade-White, A. Okumura, J. Callison, B. Brumbaugh, V. A. Avanzato, R. Rosenke, P. W. Hanley, G. Saturday, D. Scott, E. R. Fischer, E. de Wit, Respiratory disease in rhesus macaques inoculated with SARS-CoV-2. *Nature* **585**, 268-272 (2020).

12. N. B. Mercado, R. Zahn, F. Wegmann, C. Loos, A. Chandrashekar, J. Yu, J. Liu, L. Peter, K. McMahan, L. H. Tostanoski, X. He, D. R. Martinez, L. Rutten, R. Bos, D. van Manen, J. Vellinga, J. Custers, J. P. Langedijk, T. Kwaks, M. J. G. Bakkers, D. Zuijdgeest, S. K. Rosendahl Huber, C. Atyeo, S. Fischinger, J. S. Burke, J. Feldman, B. M. Hauser, T. M. Caradonna, E. A. Bondzie, G. Dagotto, M. S. Gebre, E. Hoffman, C. Jacob-Dolan, M. Kirilova, Z. Li, Z. Lin, S. H. Mahrokhian, L. F. Maxfield, F. Nampanya, R. Nityanandam, J. P. Nkolola, S. Patel, J. D. Ventura, K. Verrington, H. Wan, L. Pessaint, A. Van Ry, K. Blade, A. Strasbaugh, M. Cabus, R. Brown, A. Cook, S. Zouantchangadou, E. Teow, H. Andersen, M. G. Lewis, Y. Cai, B. Chen, A. G. Schmidt, R. K. Reeves, R. S. Baric, D. A. Lauffenburger, G. Alter, P. Stoffels, M. Mammen, J. Van Hoof, H. Schuitemaker, D. H. Barouch, Single-shot Ad26 vaccine protects against SARS-CoV-2 in rhesus macaques. *Nature* **586**, 583-588 (2020).

13. K. S. Corbett, B. Flynn, K. E. Foulds, J. R. Francica, S. Boyoglu-Barnum, A. P. Werner, B. Flach, S. O'Connell, K. W. Bock, M. Minai, B. M. Nagata, H. Andersen, D. R. Martinez, A. T. Noe, N. Douek, M. M. Donaldson, N. N. Nji, G. S. Alvarado, D. K. Edwards, D. R. Flebbe, E. Lamb, N. A. Doria-Rose, B. C. Lin, M. K. Louder, S. O'Dell, S. D. Schmidt, E. Phung, L. A. Chang, C. Yap, J. M. Todd, L. Pessaint, A. Van Ry, S. Browne, J. Greenhouse, T. Putman-Taylor, A. Strasbaugh, T. A. Campbell, A. Cook, A. Dodson, K. Steingrebe, W. Shi, Y. Zhang, O. M. Abiona, L. Wang, A. Pegu, E. S. Yang, K. Leung, T. Zhou, I. T. Teng, A. Widge, I. Gordon, L. Novik, R. A. Gillespie, R. J. Loomis, J. I. Moliva, G. Stewart-Jones, S. Himansu, W. P. Kong, M. C. Nason, K. M. Morabito, T. J. Ruckwardt, J. E. Ledgerwood, M. R. Gaudinski, P. D. Kwong, J. R. Mascola, A. Carfi, M. G. Lewis, R. S. Baric, A. McDermott, I. N. Moore, N. J. Sullivan, M. Roederer, R. A. Seder, B. S. Graham, Evaluation of the mRNA-1273 Vaccine against SARS-CoV-2 in nonhuman primates. *N Engl J Med* **383**, 1544-1555 (2020).

14. N. van Doremalen, T. Lambe, A. Spencer, S. Belij-Rammerstorfer, J. N. Purushotham, J. R. Port, V. A. Avanzato, T. Bushmaker, A. Flaxman, M. Ulaszewska, F. Feldmann, E. R. Allen, H. Sharpe, J. Schulz, M. Holbrook, A. Okumura, K. Meade-White, L. Pérez-Pérez, N. J. Edwards, D. Wright, C. Bissett, C. Gilbride, B. N. Williamson, R. Rosenke, D. Long, A. Ishwarbhai, R. Kailath, L. Rose, S. Morris, C. Powers, J. Lovaglio, P. W. Hanley, D. Scott, G. Saturday, E. de Wit, S. C. Gilbert, V. J. Munster, ChAdOx1 nCoV-19 vaccine prevents SARS-CoV-2 pneumonia in rhesus macaques. *Nature* **586**, 578-582 (2020).
15. B. N. Williamson, F. Feldmann, B. Schwarz, K. Meade-White, D. P. Porter, J. Schulz, N. van Doremalen, I. Leighton, C. K. Yinda, L. Pérez-Pérez, A. Okumura, J. Lovaglio, P. W. Hanley, G. Saturday, C. M. Bosio, S. Anzick, K. Barbian, T. Cihlar, C. Martens, D. P. Scott, V. J. Munster, E. de Wit, Clinical benefit of remdesivir in rhesus macaques infected with SARS-CoV-2. *Nature* **585**, 273-276 (2020).
16. T. Z. Song, H. Y. Zheng, J. B. Han, L. Jin, X. Yang, F. L. Liu, R. H. Luo, R. R. Tian, H. R. Cai, X. L. Feng, C. Liu, M. H. Li, Y. T. Zheng, Delayed severe cytokine storm and immune cell infiltration in SARS-CoV-2-infected aged Chinese rhesus macaques. *Zool Res* **41**, 503-516 (2020).
17. W. Enard, S. Pääbo, Comparative primate genomics. *Annu Rev Genomics Hum Genet* **5**, 351-378 (2004).
18. Z. N. Kronenberg, I. T. Fiddes, D. Gordon, S. Murali, S. Cantsilieris, O. S. Meyerson, J. G. Underwood, B. J. Nelson, M. J. P. Chaisson, M. L. Dougherty, K. M. Munson, A. R. Hastie, M. Diekhans, F. Hormozdiari, N. Lorusso, K. Hoekzema, R. Qiu, K. Clark, A. Raja, A. E. Welch, M. Sorensen, C. Baker, R. S. Fulton, J. Armstrong, T. A. Graves-Lindsay, A. M. Denli, E. R. Hoppe, P. Hsieh, C. M. Hill, A. W. C. Pang, J. Lee, E. T. Lam, S. K. Dutcher, F. H. Gage, W. C. Warren, J. Shendure, D. Haussler, V. A. Schneider, H. Cao, M. Ventura, R. K. Wilson, B. Paten, A. Pollen, E. E. Eichler, High-resolution comparative analysis of great ape genomes. *Science* **360**, eaar6343 (2018).
19. C. S. a. A. Consortium, Initial sequence of the chimpanzee genome and comparison with the human genome. *Nature* **437**, 69-87 (2005).
20. R. A. Gibbs, J. Rogers, M. G. Katze, R. Bumgarner, G. M. Weinstock, E. R. Mardis, K. A. Remington, R. L. Strausberg, J. C. Venter, R. K. Wilson, M. A. Batzer, C. D. Bustamante, E. E. Eichler, M. W. Hahn, R. C. Hardison, K. D. Makova, W. Miller, A. Milosavljevic, R. E. Palermo, A. Siepel, J. M. Sikela, T. Attaway, S. Bell, K. E. Bernard, C. J. Buhay, M. N. Chandrabose, M. Dao, C. Davis, K. D. Delehaunty, Y. Ding, H. H. Dinh, S. Dugan-Rocha, L. A. Fulton, R. A. Gabisi, T. T. Garner, J. Godfrey, A. C. Hawes, J. Hernandez, S. Hines, M. Holder, J. Hume, S. N. Jhangiani, V. Joshi, Z. M. Khan, E. F. Kirkness, A. Cree, R. G. Fowler, S. Lee, L. R. Lewis, Z. Li, Y. S. Liu, S. M. Moore, D. Muzny, L. V. Nazareth, D. N. Ngo, G. O. Okwuonu, G. Pai, D. Parker, H. A. Paul, C. Pfannkoch, C. S. Pohl, Y. H. Rogers, S. J. Ruiz, A. Sabo, J. Santibanez, B. W. Schneider, S. M. Smith, E. Sodergren, A. F. Svatek, T. R. Utterback, S. Vattathil, W. Warren, C. S. White, A. T. Chinwalla, Y. Feng, A. L. Halpern, L. W. Hillier, X. Huang, P. Minx, J. O. Nelson, K. H. Pepin, X. Qin, G. G. Sutton, E. Venter, B. P. Walenz, J. W. Wallis, K. C. Worley, S. P. Yang, S. M. Jones,

M. A. Marra, M. Rocchi, J. E. Schein, R. Baertsch, L. Clarke, M. Csürös, J. Glasscock, R. A. Harris, P. Havlak, A. R. Jackson, H. Jiang, Y. Liu, D. N. Messina, Y. Shen, H. X. Song, T. Wylie, L. Zhang, E. Birney, K. Han, M. K. Konkel, J. Lee, A. F. Smit, B. Ullmer, H. Wang, J. Xing, R. Burhans, Z. Cheng, J. E. Karro, J. Ma, B. Raney, X. She, M. J. Cox, J. P. Demuth, L. J. Dumas, S. G. Han, J. Hopkins, A. Karimpour-Fard, Y. H. Kim, J. R. Pollack, T. Vinar, C. Addo-Quaye, J. Degenhardt, A. Denby, M. J. Hubisz, A. Indap, C. Kosiol, B. T. Lahn, H. A. Lawson, A. Marklein, R. Nielsen, E. J. Vallender, A. G. Clark, B. Ferguson, R. D. Hernandez, K. Hirani, H. Kehrer-Sawatzki, J. Kolb, S. Patil, L. L. Pu, Y. Ren, D. G. Smith, D. A. Wheeler, I. Schenck, E. V. Ball, R. Chen, D. N. Cooper, B. Giardine, F. Hsu, W. J. Kent, A. Lesk, D. L. Nelson, E. O'Brien W, K. Prüfer, P. D. Stenson, J. C. Wallace, H. Ke, X. M. Liu, P. Wang, A. P. Xiang, F. Yang, G. P. Barber, D. Haussler, D. Karolchik, A. D. Kern, R. M. Kuhn, K. E. Smith, A. S. Zwieg, Evolutionary and biomedical insights from the rhesus macaque genome. *Science* **316**, 222-234 (2007).

21. A. Scally, J. Y. Dutheil, L. W. Hillier, G. E. Jordan, I. Goodhead, J. Herrero, A. Hobolth, T. Lappalainen, T. Mailund, T. Marques-Bonet, S. McCarthy, S. H. Montgomery, P. C. Schwalie, Y. A. Tang, M. C. Ward, Y. Xue, B. Yngvadottir, C. Alkan, L. N. Andersen, Q. Ayub, E. V. Ball, K. Beal, B. J. Bradley, Y. Chen, C. M. Clee, S. Fitzgerald, T. A. Graves, Y. Gu, P. Heath, A. Heger, E. Karakoc, A. Kolb-Kokocinski, G. K. Laird, G. Lunter, S. Meader, M. Mort, J. C. Mullikin, K. Munch, T. D. O'Connor, A. D. Phillips, J. Prado-Martinez, A. S. Rogers, S. Sajjadian, D. Schmidt, K. Shaw, J. T. Simpson, P. D. Stenson, D. J. Turner, L. Vigilant, A. J. Vilella, W. Whitener, B. Zhu, D. N. Cooper, P. de Jong, E. T. Dermitzakis, E. E. Eichler, P. Flicek, N. Goldman, N. I. Mundy, Z. Ning, D. T. Odom, C. P. Ponting, M. A. Quail, O. A. Ryder, S. M. Searle, W. C. Warren, R. K. Wilson, M. H. Schierup, J. Rogers, C. Tyler-Smith, R. Durbin, Insights into hominid evolution from the gorilla genome sequence. *Nature* **483**, 169-175 (2012).

22. M. G. S. a. A. Consortium, The common marmoset genome provides insight into primate biology and evolution. *Nat Genet* **46**, 850-857 (2014).

23. D. P. Locke, L. W. Hillier, W. C. Warren, K. C. Worley, L. V. Nazareth, D. M. Muzny, S. P. Yang, Z. Wang, A. T. Chinwalla, P. Minx, M. Mitreva, L. Cook, K. D. Delehaunty, C. Fronick, H. Schmidt, L. A. Fulton, R. S. Fulton, J. O. Nelson, V. Magrini, C. Pohl, T. A. Graves, C. Markovic, A. Cree, H. H. Dinh, J. Hume, C. L. Kovar, G. R. Fowler, G. Lunter, S. Meader, A. Heger, C. P. Ponting, T. Marques-Bonet, C. Alkan, L. Chen, Z. Cheng, J. M. Kidd, E. E. Eichler, S. White, S. Searle, A. J. Vilella, Y. Chen, P. Flicek, J. Ma, B. Raney, B. Suh, R. Burhans, J. Herrero, D. Haussler, R. Faria, O. Fernando, F. Darré, D. Farré, E. Gazave, M. Oliva, A. Navarro, R. Roberto, O. Capozzi, N. Archidiacono, G. Della Valle, S. Purgato, M. Rocchi, M. K. Konkel, J. A. Walker, B. Ullmer, M. A. Batzer, A. F. Smit, R. Hubley, C. Casola, D. R. Schrider, M. W. Hahn, V. Quesada, X. S. Puente, G. R. Ordoñez, C. López-Otín, T. Vinar, B. Brejova, A. Ratan, R. S. Harris, W. Miller, C. Kosiol, H. A. Lawson, V. Taliwal, A. L. Martins, A. Siepel, A. Roychoudhury, X. Ma, J. Degenhardt, C. D. Bustamante, R. N. Gutenkunst, T. Mailund, J. Y. Dutheil, A. Hobolth, M. H. Schierup, O. A. Ryder, Y. Yoshinaga, P. J. de Jong, G. M.

Weinstock, J. Rogers, E. R. Mardis, R. A. Gibbs, R. K. Wilson, Comparative and demographic analysis of orangutan genomes. *Nature* **469**, 529-533 (2011).
24. L. Carbone, R. A. Harris, S. Gnerre, K. R. Veeramah, B. Lorente-Galdos, J. Huddleston, T. J. Meyer, J. Herrero, C. Roos, B. Aken, F. Anaclerio, N. Archidiacono, C. Baker, D. Barrell, M. A. Batzer, K. Beal, A. Blancher, C. L. Bohrson, M. Brameier, M. S. Campbell, O. Capozzi, C. Casola, G. Chiatante, A. Cree, A. Damert, P. J. de Jong, L. Dumas, M. Fernandez-Callejo, P. Flicek, N. V. Fuchs, I. Gut, M. Gut, M. W. Hahn, J. Hernandez-Rodriguez, L. W. Hillier, R. Hubley, B. Ianc, Z. Izsvák, N. G. Jablonski, L. M. Johnstone, A. Karimpour-Fard, M. K. Konkel, D. Kostka, N. H. Lazar, S. L. Lee, L. R. Lewis, Y. Liu, D. P. Locke, S. Mallick, F. L. Mendez, M. Muffato, L. V. Nazareth, K. A. Nevonen, M. O'Bleness, C. Ochis, D. T. Odom, K. S. Pollard, J. Quilez, D. Reich, M. Rocchi, G. G. Schumann, S. Searle, J. M. Sikela, G. Skollar, A. Smit, K. Sonmez, B. ten Hallers, E. Terhune, G. W. Thomas, B. Ullmer, M. Ventura, J. A. Walker, J. D. Wall, L. Walter, M. C. Ward, S. J. Wheelan, C. W. Whelan, S. White, L. J. Wilhelm, A. E. Woerner, M. Yandell, B. Zhu, M. F. Hammer, T. Marques-Bonet, E. E. Eichler, L. Fulton, C. Fronick, D. M. Muzny, W. C. Warren, K. C. Worley, J. Rogers, R. K. Wilson, R. A. Gibbs, Gibbon genome and the fast karyotype evolution of small apes. *Nature* **513**, 195-201 (2014).
25. L. Yu, G. D. Wang, J. Ruan, Y. B. Chen, C. P. Yang, X. Cao, H. Wu, Y. H. Liu, Z. L. Du, X. P. Wang, J. Yang, S. C. Cheng, L. Zhong, L. Wang, X. Wang, J. Y. Hu, L. Fang, B. Bai, K. L. Wang, N. Yuan, S. F. Wu, B. G. Li, J. G. Zhang, Y. Q. Yang, C. L. Zhang, Y. C. Long, H. S. Li, J. Y. Yang, D. M. Irwin, O. A. Ryder, Y. Li, C. I. Wu, Y. P. Zhang, Genomic analysis of snub-nosed monkeys (*Rhinopithecus*) identifies genes and processes related to high-altitude adaptation. *Nat Genet* **48**, 947-952 (2016).
26. X. Zhou, B. Wang, Q. Pan, J. Zhang, S. Kumar, X. Sun, Z. Liu, H. Pan, Y. Lin, G. Liu, W. Zhan, M. Li, B. Ren, X. Ma, H. Ruan, C. Cheng, D. Wang, F. Shi, Y. Hui, Y. Tao, C. Zhang, P. Zhu, Z. Xiang, W. Jiang, J. Chang, H. Wang, Z. Cao, Z. Jiang, B. Li, G. Yang, C. Roos, P. A. Garber, M. W. Bruford, R. Li, M. Li, Whole-genome sequencing of the snub-nosed monkey provides insights into folivory and evolutionary history. *Nat Genet* **46**, 1303-1310 (2014).
27. A. O. Ayoola, B. L. Zhang, R. P. Meisel, L. M. Nneji, Y. Shao, O. B. Morenikeji, A. C. Adeola, S. I. Ng'ang'a, B. G. Ogunjemite, A. O. Okeyoyin, C. Roos, D. D. Wu, Population genomics reveals incipient speciation, introgression, and adaptation in the African mona monkey (*Cercopithecus mona*). *Mol Biol Evol* **38**, 876-890 (2021).
28. D. M. Bickhart, B. D. Rosen, S. Koren, B. L. Sayre, A. R. Hastie, S. Chan, J. Lee, E. T. Lam, I. Liachko, S. T. Sullivan, J. N. Burton, H. J. Huson, J. C. Nystrom, C. M. Kelley, J. L. Hutchison, Y. Zhou, J. Sun, A. Crisa, F. A. Ponce de Leon, J. C. Schwartz, J. A. Hammond, G. C. Waldbieser, S. G. Schroeder, G. E. Liu, M. J. Dunham, J. Shendure, T. S. Sonstegard, A. M. Phillippy, C. P. Van Tassell, T. P. Smith, Single-molecule sequencing and chromatin conformation capture enable *de novo* reference assembly of the domestic goat genome. *Nat Genet* **49**, 643-650 (2017).

29. B.-L. Zhang., W. Chen., Z. Wang., W. Pang., M.-T. Luo., S. Wang., Y. Shao., W.-Q. He., Y. Deng., L. Zhou., J. Chen., M. Yang., Y. Wu., L. Wang., H. Fernandez., S. Molloy., H. Meunier., F. Wanert., L. Kuderna., T. Marques-Bonet., C. Roos., X. Qi., M. Li., Z.-J. Liu., M. H. Schierup., D. N. Cooper., J. Liu., Y.-T. Zheng., G. Zhang., D.-D. Wu., Comparative genomics reveals the hybrid origin of a macaque group. *Sci Adv*, accepted (2022).
30. H. Wu., Z. Wang., Y. Zhang., L. Frantz., C. Roos., D. M. Irwin., C. Zhang., X. Liu., D. Wu., S. Huang., T. Gu., J. Liu., L. Yu., Hybrid origin of a primate, the gray snub-nosed monkey. *Science*, accepted (2022).
31. J. Wu., L. Zhao., L. Wang., X. Guang., P. A. Garber., C. Opie., Y. Yuan., R. Diao., G. Li., K. Wang., R. Pan., W. Ji., H. Sun., Z.-P. Huang., C. Xu., A. B. Witarto., R. Jia., C. Zhang., C. Deng., Q. Qiu., G. Zhang., Cyril C. Grueter, D.-D. Wu., B. Li., X.-G. Qi., Cold adaptations promoted social evolution in Asian Colobine Primate. *Science*, accepted (2022).
32. Ming-Li Li, Sheng Wang, Penghui Xu, Hang-Yu Tian , Yong Shao, Zi-Jun Xiong, Xiao-Guang Qi, David N. Cooper, Ya-Ping Zhang, Guojie Zhang, He Helen Zhu, D.-D. Wu, Functional genomics analysis reveals the evolutionary adaptation and demographic history of *pygmy lorises*. *Proc Natl Acad Sci U S A* **119**, e2123030119 (2022).
33. M. S. Ye, J. Y. Zhang, D. D. Yu, M. Xu, L. Xu, L. B. Lv, Q. Y. Zhu, Y. Fan, Y. G. Yao, Comprehensive annotation of the Chinese tree shrew genome by large-scale RNA sequencing and long-read isoform sequencing. *Zool Res* **42**, 692-709 (2021).
34. A. M. Kozlov, A. J. Aberer, A. Stamatakis, ExaML version 3: a tool for phylogenomic analyses on supercomputers. *Bioinformatics* **31**, 2577-2579 (2015).
35. P. Perelman, W. E. Johnson, C. Roos, H. N. Seuánez, J. E. Horvath, M. A. Moreira, B. Kessing, J. Pontius, M. Roelke, Y. Rumpler, M. P. Schneider, A. Silva, S. J. O'Brien, J. Pecon-Slattery, A molecular phylogeny of living primates. *PLoS Genet* **7**, e1001342 (2011).
36. C. M. Shi, Z. Yang, Coalescent-based analyses of genomic sequence data provide a robust resolution of phylogenetic relationships among major groups of gibbons. *Mol Biol Evol* **35**, 159-179 (2018).
37. A. Hobolth, O. F. Christensen, T. Mailund, M. H. Schierup, Genomic relationships and speciation times of human, chimpanzee, and gorilla inferred from a coalescent hidden Markov model. *PLoS Genet* **3**, e7 (2007).
38. I. Rivas-González., M. Rousselle., F. Li., L. Zhou., J. Y. Dutheil., K. Munch., Y. Shao., D. Wu., M. H. Schierup., G. Zhang., Pervasive incomplete lineage sorting illuminates speciation and selection processes in primates. *Science*, under review (2022).
39. D. Vanderpool, B. Q. Minh, R. Lanfear, D. Hughes, S. Murali, R. A. Harris, M. Raveendran, D. M. Muzny, M. S. Hibbins, R. J. Williamson, Primate phylogenomics uncovers multiple rapid radiations and ancient interspecific introgression. *PLoS Biol* **18**, e3000954 (2020).
40. Z. Yang, PAML 4: phylogenetic analysis by maximum likelihood. *Mol Biol Evol* **24**, 1586-1591 (2007).

41. S. Alvarez-Carretero, A. U. Tamuri, M. Battini, F. F. Nascimento, E. Carlisle, R. J. Asher, Z. Yang, P. C. J. Donoghue, M. Dos Reis, A species-level timeline of mammal evolution integrating phylogenomic data. *Nature* **602**, 263-267 (2022).
42. C. Liu, J. Gao, X. Cui, Z. Li, L. Chen, Y. Yuan, Y. Zhang, L. Mei, L. Zhao, D. Cai, M. Hu, B. Zhou, Z. Li, T. Qin, H. Si, G. Li, Z. Lin, Y. Xu, C. Zhu, Y. Yin, C. Zhang, W. Xu, Q. Li, K. Wang, M. T. P. Gilbert, R. Heller, W. Wang, J. Huang, Q. Qiu, A towering genome: Experimentally validated adaptations to high blood pressure and extreme stature in the giraffe. *Sci Adv* **7**, eabe9459 (2021).
43. E. E. Eichler, D. Sankoff, Structural dynamics of eukaryotic chromosome evolution. *Science* **301**, 793-797 (2003).
44. Y. Yin, H. Fan, B. Zhou, Y. Hu, G. Fan, J. Wang, F. Zhou, W. Nie, C. Zhang, L. Liu, Z. Zhong, W. Zhu, G. Liu, Z. Lin, C. Liu, J. Zhou, G. Huang, Z. Li, J. Yu, Y. Zhang, Y. Yang, B. Zhuo, B. Zhang, J. Chang, H. Qian, Y. Peng, X. Chen, L. Chen, Z. Li, Q. Zhou, W. Wang, F. Wei, Molecular mechanisms and topological consequences of drastic chromosomal rearrangements of muntjac deer. *Nat Commun* **12**, 6858 (2021).
45. R. Stanyon, M. Rocchi, O. Capozzi, R. Roberto, D. Misceo, M. Ventura, M. F. Cardone, F. Bigoni, N. Archidiacono, Primate chromosome evolution: ancestral karyotypes, marker order and neocentromeres. *Chromosome Res* **16**, 17-39 (2008).
46. T. Marques-Bonet, J. M. Kidd, M. Ventura, T. A. Graves, Z. Cheng, L. W. Hillier, Z. Jiang, C. Baker, R. Malfavon-Borja, L. A. Fulton, C. Alkan, G. Aksay, S. Girirajan, P. Siswara, L. Chen, M. F. Cardone, A. Navarro, E. R. Mardis, R. K. Wilson, E. E. Eichler, A burst of segmental duplications in the genome of the African great ape ancestor. *Nature* **457**, 877-881 (2009).
47. P. D. Stenson., M. Mort., E. V. Ball., M. Chapman., K. Evans., L. Azevedo., M. Hayden., S. Heywood., D. S. Millar., A. D. Phillips., D. N. Cooper., The Human Gene Mutation Database (HGMD ®): optimizing its use in a clinical diagnostic or research setting. *Hum Genet* **139**, 1197-1207 (2020).
48. L. Chen, Q. Qiu, Y. Jiang, K. Wang, Z. Lin, Z. Li, F. Bibi, Y. Yang, J. Wang, W. Nie, W. Su, G. Liu, Q. Li, W. Fu, X. Pan, C. Liu, J. Yang, C. Zhang, Y. Yin, Y. Wang, Y. Zhao, C. Zhang, Z. Wang, Y. Qin, W. Liu, B. Wang, Y. Ren, R. Zhang, Y. Zeng, R. R. da Fonseca, B. Wei, R. Li, W. Wan, R. Zhao, W. Zhu, Y. Wang, S. Duan, Y. Gao, Y. E. Zhang, C. Chen, C. Hvilsom, C. W. Epps, L. G. Chemnick, Y. Dong, S. Mirarab, H. R. Siegismund, O. A. Ryder, M. T. P. Gilbert, H. A. Lewin, G. Zhang, R. Heller, W. Wang, Large-scale ruminant genome sequencing provides insights into their evolution and distinct traits. *Science* **364**, eaav6202 (2019).
49. J. D. Smith, J. W. Bickham, T. R. Gregory, Patterns of genome size diversity in bats (order Chiroptera). *Genome* **56**, 457-472 (2013).
50. S. Shen, L. Lin, J. J. Cai, P. Jiang, E. J. Kenkel, M. R. Stroik, S. Sato, B. L. Davidson, Y. Xing, Widespread establishment and regulatory impact of Alu exons in human genes. *Proc Natl Acad Sci U S A* **108**, 2837-2842 (2011).
51. G. E. Liu, C. Alkan, L. Jiang, S. Zhao, E. E. Eichler, Comparative analysis of Alu repeats in primate genomes. *Genome Res* **19**, 876-885 (2009).

52. T. Hayakawa, Y. Satta, P. Gagneux, A. Varki, N. Takahata, Alu-mediated inactivation of the human CMP-*N*-acetylneuraminic acid hydroxylase gene. *Proc Natl Acad Sci U S A* **98**, 11399-11404 (2001).
53. P. Kuehnen, M. Mischke, S. Wiegand, C. Sers, B. Horsthemke, S. Lau, T. Keil, Y. A. Lee, A. Grueters, H. Krude, An Alu element-associated hypermethylation variant of the *POMC* gene is associated with childhood obesity. *PLoS Genet* **8**, e1002543 (2012).
54. J. Jurka, Evolutionary impact of human Alu repetitive elements. *Curr Opin Genet Dev* **14**, 603-608 (2004).
55. G. Zhang, C. Li, Q. Li, B. Li, D. M. Larkin, C. Lee, J. F. Storz, A. Antunes, M. J. Greenwold, R. W. Meredith, A. Ödeen, J. Cui, Q. Zhou, L. Xu, H. Pan, Z. Wang, L. Jin, P. Zhang, H. Hu, W. Yang, J. Hu, J. Xiao, Z. Yang, Y. Liu, Q. Xie, H. Yu, J. Lian, P. Wen, F. Zhang, H. Li, Y. Zeng, Z. Xiong, S. Liu, L. Zhou, Z. Huang, N. An, J. Wang, Q. Zheng, Y. Xiong, G. Wang, B. Wang, J. Wang, Y. Fan, R. R. da Fonseca, A. Alfaro-Núñez, M. Schubert, L. Orlando, T. Mourier, J. T. Howard, G. Ganapathy, A. Pfenning, O. Whitney, M. V. Rivas, E. Hara, J. Smith, M. Farré, J. Narayan, G. Slavov, M. N. Romanov, R. Borges, J. P. Machado, I. Khan, M. S. Springer, J. Gatesy, F. G. Hoffmann, J. C. Opazo, O. Håstad, R. H. Sawyer, H. Kim, K. W. Kim, H. J. Kim, S. Cho, N. Li, Y. Huang, M. W. Bruford, X. Zhan, A. Dixon, M. F. Bertelsen, E. Derryberry, W. Warren, R. K. Wilson, S. Li, D. A. Ray, R. E. Green, S. J. O'Brien, D. Griffin, W. E. Johnson, D. Haussler, O. A. Ryder, E. Willerslev, G. R. Graves, P. Alström, J. Fjeldså, D. P. Mindell, S. V. Edwards, E. L. Braun, C. Rahbek, D. W. Burt, P. Houde, Y. Zhang, H. Yang, J. Wang, E. D. Jarvis, M. T. Gilbert, J. Wang, Comparative genomics reveals insights into avian genome evolution and adaptation. *Science* **346**, 1311-1320 (2014).
56. P. Moorjani, C. E. Amorim, P. F. Arndt, M. Przeworski, Variation in the molecular clock of primates. *Proc Natl Acad Sci U S A* **113**, 10607-10612 (2016).
57. E. Fontanillas, J. J. Welch, J. A. Thomas, L. Bromham, The influence of body size and net diversification rate on molecular evolution during the radiation of animal phyla. *BMC Evol Biol* **7**, 95 (2007).
58. A. Wong, Covariance between testes size and substitution rates in primates. *Mol Biol Evol* **31**, 1432-1436 (2014).
59. W. H. Li, M. Tanimura, The molecular clock runs more slowly in man than in apes and monkeys. *Nature* **326**, 93-96 (1987).
60. M. E. Steiper, N. M. Young, Primate molecular divergence dates. *Mol Phylogenet Evol* **41**, 384-394 (2006).
61. S. H. Kim, N. Elango, C. Warden, E. Vigoda, S. V. Yi, Heterogeneous genomic molecular clocks in primates. *PLoS Genet* **2**, e163 (2006).
62. J. Schmitz, A. Noll, C. A. Raabe, G. Churakov, R. Voss, M. Kiefmann, T. Rozhdestvensky, J. Brosius, R. Baertsch, H. Clawson, C. Roos, A. Zimin, P. Minx, M. J. Montague, R. K. Wilson, W. C. Warren, Genome sequence of the basal haplorrhine primate *Tarsius syrichta* reveals unusual insertions. *Nat Commun* **7**, 12997 (2016).

63. L. Fang, W. Cai, S. Liu, O. Canela-Xandri, Y. Gao, J. Jiang, K. Rawlik, B. Li, S. G. Schroeder, B. D. Rosen, C. J. Li, T. S. Sonstegard, L. J. Alexander, C. P. Van Tassell, P. M. VanRaden, J. B. Cole, Y. Yu, S. Zhang, A. Tenesa, L. Ma, G. E. Liu, Comprehensive analyses of 723 transcriptomes enhance genetic and biological interpretations for complex traits in cattle. *Genome Res* **30**, 790-801 (2020).
64. B. Y. Liao, J. Zhang, Low rates of expression profile divergence in highly expressed genes and tissue-specific genes during mammalian evolution. *Mol Biol Evol* **23**, 1119-1128 (2006).
65. G. J. Wyckoff, W. Wang, C. I. Wu, Rapid evolution of male reproductive genes in the descent of man. *Nature* **403**, 304-309 (2000).
66. T. Boehm, Evolution of vertebrate immunity. *Curr Biol* **22**, R722-R732 (2012).
67. H. Y. Wang, H. C. Chien, N. Osada, K. Hashimoto, S. Sugano, T. Gojobori, C. K. Chou, S. F. Tsai, C. I. Wu, C. K. Shen, Rate of evolution in brain-expressed genes in humans and other primates. *PLoS Biol* **5**, e13 (2007).
68. Materials and methods are available as Supplementary Material.
69. J. Tohyama, M. Nakashima, S. Nabatame, C. n. Gaik-Siew, R. Miyata, Z. Rener-Primec, M. Kato, N. Matsumoto, H. Saitsu, *SPTAN1* encephalopathy: distinct phenotypes and genotypes. *J Hum Genet* **60**, 167-173 (2015).
70. P. Mansfield, J. N. Constantino, D. Baldridge, *MYT1L*: A systematic review of genetic variation encompassing schizophrenia and autism. *Am J Med Genet B Neuropsychiatr Genet* **183**, 227-233 (2020).
71. M. Maekawa, T. Ohnishi, K. Hashimoto, A. Watanabe, Y. Iwayama, H. Ohba, E. Hattori, K. Yamada, T. Yoshikawa, Analysis of strain-dependent prepulse inhibition points to a role for Shmt1 (*SHMT1*) in mice and in schizophrenia. *J Neurochem* **115**, 1374-1385 (2010).
72. X. Bi., L. Zhou., J.-J. Zhang., S. Feng., M. Hu., D. N. Cooper., J. Lin., J. Li., D.-D. Wu., G. Zhang., Lineage-specific accelerated sequences underlying primate evolution. *Sci adv*, under review (2022).
73. J. K. Rilling, T. R. Insel, Differential expansion of neural projection systems in primate brain evolution. *Neuroreport* **10**, 1453-1459 (1999).
74. K. Isler, E. Christopher Kirk, J. M. Miller, G. A. Albrecht, B. R. Gelvin, R. D. Martin, Endocranial volumes of primate species: scaling analyses using a comprehensive and reliable data set. *J Hum Evol* **55**, 967-978 (2008).
75. C. Plachez, L. J. Richards, Mechanisms of axon guidance in the developing nervous system. *Curr Top Dev Biol* **69**, 267-346 (2005).
76. M. A. Robichaux, C. W. Cowan, Signaling mechanisms of axon guidance and early synaptogenesis. *Curr Top Behav Neurosci* **16**, 19-48 (2014).
77. J. Falk, A. Bechara, R. Fiore, H. Nawabi, H. Zhou, C. Hoyo-Becerra, M. Bozon, G. Rougon, M. Grumet, A. W. Puschel, J. R. Sanes, V. Castellani, Dual functional activity of semaphorin 3B is required for positioning the anterior commissure. *Neuron* **48**, 63-75 (2005).
78. M. A. Wolman, Y. Liu, H. Tawarayama, W. Shoji, M. C. Halloran, Repulsion and attraction of axons by semaphorin3D are mediated by different neuropilins in vivo. *J Neurosci* **24**, 8428-8435 (2004).

79. C. Kudo, I. Ajioka, Y. Hirata, K. Nakajima, Expression profiles of *EPHA3* at both the RNA and protein level in the developing mammalian forebrain. *J Comp Neurol* **487**, 255-269 (2005).
80. M. V. Tejada-Simon, Modulation of actin dynamics by *RAC1* to target cognitive function. *J Neurochem* **133**, 767-779 (2015).
81. S. L. Eastwood, P. J. Harrison, Decreased mRNA Expression of Netrin-G1 and Netrin-G2 in the Temporal Lobe in Schizophrenia and Bipolar Disorder. *Neuropsychopharmacology* **33**, 933-945 (2008).
82. D. Pan, Hippo signaling in organ size control. *Genes Dev* **21**, 886-897 (2007).
83. S. H. Patel, F. D. Camargo, D. Yimlamai, Hippo signaling in the liver regulates organ size, cell fate, and carcinogenesis. *Gastroenterology* **152**, 533-545 (2017).
84. R. H. Gokhale, A. W. Shingleton, Size control: the developmental physiology of body and organ size regulation. *Wiley Interdiscip Rev Dev Biol* **4**, 335-356 (2015).
85. E. C. Kirk, Comparative morphology of the eye in primates. *Anat Rec A Discov Mol Cell Evol Biol* **281**, 1095-1103 (2004).
86. A. C. Wiik, C. Wade, T. Biagi, E. O. Ropstad, E. Bjerkas, K. Lindblad-Toh, F. Lingaas, A deletion in nephronophthisis 4 (*NPHP4*) is associated with recessive cone-rod dystrophy in standard wire-haired dachshund. *Genome Res* **18**, 1415-1421 (2008).
87. P. Liskova, L. Dudakova, C. J. Evans, K. E. Rojas Lopez, N. Pontikos, D. Athanasiou, H. Jama, J. Sach, P. Skalicka, V. Stranecky, S. Kmoch, C. Thaung, M. Filipec, M. E. Cheetham, A. E. Davidson, S. J. Tuft, A. J. Hardcastle, Ectopic *GRHL2* expression due to non-coding mutations promotes cell state transition and causes posterior polymorphous corneal dystrophy 4. *Am J Hum Genet* **102**, 447-459 (2018).
88. Y. Toda, T. Hayakawa, A. Itoigawa, Y. Kurihara, T. Nakagita, M. Hayashi, R. Ashino, A. D. Melin, Y. Ishimaru, S. Kawamura, H. Imai, T. Misaka, Evolution of the primate glutamate taste sensor from a nucleotide sensor. *Curr Biol* **31**, 4641-4649.e4645 (2021).
89. J. M. Kamilar, B. J. Bradley, Interspecific variation in primate coat colour supports Gloger's rule. *J Biogeogr* **38**, 2270-2277 (2011).
90. S. Hu, Y. Chen, B. Zhao, N. Yang, S. Chen, J. Shen, G. Bao, X. Wu, *KIT* is involved in melanocyte proliferation, apoptosis and melanogenesis in the rex rabbit. *PeerJ* **8**, e9402 (2020).
91. M. C. Garrido, B. C. Bastian, *KIT* as a therapeutic target in melanoma. *J Invest Dermatol* **130**, 20-27 (2010).
92. J. M. Grichnik, KIT and melanocyte migration. *J Invest Dermatol* **126**, 945-947 (2006).
93. Y. Mizutani, N. Hayashi, M. Kawashima, G. Imokawa, A single UVB exposure increases the expression of functional *KIT* in human melanocytes by up-regulating *MITF* expression through the phosphorylation of p38/CREB. *Arch Dermatol Res* **302**, 283-294 (2010).
94. R. Kitamura, K. Tsukamoto, K. Harada, A. Shimizu, S. Shimada, T. Kobayashi, G. Imokawa, Mechanisms underlying the dysfunction of melanocytes in vitiligo

epidermis: role of SCF/KIT protein interactions and the downstream effector, MITF-M. *J Pathol* **202**, 463-475 (2004).
95. B. Wen, Y. Chen, H. Li, J. Wang, J. Shen, A. Ma, J. Qu, K. Bismuth, J. Debbache, H. Arnheiter, L. Hou, Allele-specific genetic interactions between Mitf and Kit affect melanocyte development. *Pigment Cell Melanoma Res* **23**, 441-447 (2010).
96. D. L. C. van den Berg, R. Azzarelli, K. Oishi, B. Martynoga, N. Urban, D. H. W. Dekkers, J. A. Demmers, F. Guillemot, *NIPBL* interacts with *ZFP609* and the integrator complex to regulate cortical neuron migration. *Neuron* **93**, 348-361 (2017).
97. G. H. Mochida, C. A. Walsh, Molecular genetics of human microcephaly. *Curr Opin Neurol* **14**, 151-156 (2001).
98. S. H. Montgomery, I. Capellini, C. Venditti, R. A. Barton, N. I. Mundy, Adaptive evolution of four microcephaly genes and the evolution of brain size in Anthropoid primates. *Mol Biol Evol* **28**, 625-638 (2010).
99. L. Shi, M. Li, Q. Lin, X. Qi, B. Su, Functional divergence of the brain-size regulating gene *MCPH1* during primate evolution and the origin of humans. *BMC Biol* **11**, 62 (2013).
100. L. Shi, B. Su, A transgenic monkey model for the study of human brain evolution. *Zool Res* **40**, 236-238 (2019).
101. J. Rogers, P. Kochunov, K. Zilles, W. Shelledy, J. Lancaster, P. Thompson, R. Duggirala, J. Blangero, P. T. Fox, D. C. Glahn, On the genetic architecture of cortical folding and brain volume in primates. *Neuroimage* **53**, 1103-1108 (2010).
102. S. V. Puram, A. Riccio, S. Koirala, Y. Ikeuchi, A. H. Kim, G. Corfas, A. Bonni, A TRPC5-regulated calcium signaling pathway controls dendrite patterning in the mammalian brain. *Genes Dev* **25**, 2659-2673 (2011).
103. A. Yamada, E. Inoue, M. Deguchi-Tawarada, C. Matsui, A. Togawa, T. Nakatani, Y. Ono, Y. Takai, *NECL-2*/*CADM1* interacts with *ERBB4* and regulates its activity in GABAergic neurons. *Mol Cell Neurosci* **56**, 234-243 (2013).
104. R. Kusano, K. Fujita, Y. Shinoda, Y. Nagaura, H. Kiyonari, T. Abe, T. Watanabe, Y. Matsui, M. Fukaya, H. Sakagami, T. Sato, J.-i. Funahashi, M. Ohnishi, S. Tamura, T. Kobayashi, Targeted disruption of the mouse protein phosphatase *PPM1L* gene leads to structural abnormalities in the brain. *FEBS Letters* **590**, 3606-3615 (2016).
105. M. Talarowska, J. Szemraj, M. Kowalczyk, P. Gałecki, Serum *KIBRA* mRNA and protein expression and cognitive functions in depression. *Med Sci Monit* **22**, 152-160 (2016).
106. A. K. Pandey, L. Lu, X. Wang, R. Homayouni, R. W. Williams, Functionally enigmatic genes: a case study of the brain ignorome. *PLoS One* **9**, e88889 (2014).
107. A. Graziano, G. Foffani, E. B. Knudsen, J. Shumsky, K. A. Moxon, Passive exercise of the hind limbs after complete thoracic transection of the spinal cord promotes cortical reorganization. *PLoS One* **8**, e54350 (2013).
108. H. Li, J. C. Radford, M. J. Ragusa, K. L. Shea, S. R. McKercher, J. D. Zaremba, W. Soussou, Z. Nie, Y. J. Kang, N. Nakanishi, S. Okamoto, A. J. Roberts, J. J. Schwarz, S. A. Lipton, Transcription factor *MEF2C* influences neural stem/progenitor cell differentiation and maturation *in vivo*. *Proc Natl Acad Sci U S A* **105**, 9397-9402 (2008).

109. Y. Chang, O. Klezovitch, R. S. Walikonis, V. Vasioukhin, J. J. LoTurco, Discs large 5 is required for polarization of citron kinase in mitotic neural precursors. *Cell Cycle* **9**, 1990-1997 (2010).
110. M. R. Sarkisian, Discs large 5: a new regulator of Citron kinase localization in developing neocortex: comment on: Chang Y, et al. Cell Cycle 2010; 9:1990-7. *Cell Cycle* **9**, 1876 (2010).
111. D. A. Berg, L. Belnoue, H. Song, A. Simon, Neurotransmitter-mediated control of neurogenesis in the adult vertebrate brain. *Development* **140**, 2548-2561 (2013).
112. P. Levitt, J. A. Harvey, E. Friedman, K. Simansky, E. H. Murphy, New evidence for neurotransmitter influences on brain development. *Trends Neurosci* **20**, 269-274 (1997).
113. L. Wang, X. You, S. Lotinun, L. Zhang, N. Wu, W. Zou, Mechanical sensing protein PIEZO1 regulates bone homeostasis via osteoblast-osteoclast crosstalk. *Nat Commun* **11**, 282 (2020).
114. M. Linder, M. Hecking, E. Glitzner, K. Zwerina, M. Holcmann, L. Bakiri, M. G. Ruocco, J. Tuckermann, G. Schett, E. F. Wagner, M. Sibilia, *EGFR* controls bone development by negatively regulating mTOR-signaling during osteoblast differentiation. *Cell Death Differ* **25**, 1094-1106 (2018).
115. F. Xiao, C. Wang, C. Wang, Y. Gao, X. Zhang, X. Chen, *BMPER* enhances bone formation by promoting the osteogenesis-angiogenesis coupling process in mesenchymal stem cells. *Cell Physiol Biochem* **45**, 1927-1939 (2018).
116. S. Zanotti, E. Canalis, *NOTCH1* and *NOTCH2* expression in osteoblast precursors regulates femoral microarchitecture. *Bone* **62**, 22-28 (2014).
117. J. M. Kim, C. Lin, Z. Stavre, M. B. Greenblatt, J. H. Shim, Osteoblast-osteoclast communication and bone homeostasis. *Cells* **9**, 2073 (2020).
118. S. Zanotti, E. Canalis, Notch signaling and the skeleton. *Endocr Rev* **37**, 223-253 (2016).
119. M. Schmidt, Locomotion and postural behaviour. *Adv Sci Res* **5**, 23-39 (2011).
120. Y. He, X. Luo, B. Zhou, T. Hu, X. Meng, P. A. Audano, Z. N. Kronenberg, E. E. Eichler, J. Jin, Y. Guo, Y. Yang, X. Qi, B. Su, Long-read assembly of the Chinese rhesus macaque genome and identification of ape-specific structural variants. *Nat Commun* **10**, 4233 (2019).
121. S. A. Williams, G. A. Russo, Evolution of the hominoid vertebral column: the long and the short of it. *Evol Anthropol* **24**, 15-32 (2015).
122. K. Semba, K. Araki, Z. Li, K. Matsumoto, M. Suzuki, N. Nakagata, K. Takagi, M. Takeya, K. Yoshinobu, M. Araki, K. Imai, K. Abe, K. Yamamura, A novel murine gene, sickle tail, linked to the Danforth's short tail locus, is required for normal development of the intervertebral disc. *Genetics* **172**, 445-456 (2006).
123. N. Al Dhaheri, N. Wu, S. Zhao, Z. Wu, R. D. Blank, J. Zhang, C. Raggio, M. Halanski, J. Shen, K. Noonan, G. Qiu, B. Nemeth, S. Sund, S. L. Dunwoodie, G. Chapman, I. Glurich, R. D. Steiner, E. Wohler, R. Martin, N. L. Sobreira, P. F. Giampietro, *KIAA1217*: a novel candidate gene associated with isolated and syndromic vertebral malformations. *Am J Med Genet A* **182**, 1664-1672 (2020).

124. J. R. Usherwood, J. E. Bertram, Understanding brachiation: insight from a collisional perspective. *J Exp Biol* **206**, 1631-1642 (2003).
125. J. R. Usherwood, S. G. Larson, J. E. Bertram, Mechanisms of force and power production in unsteady ricochetal brachiation. *Am J Phys Anthropol* **120**, 364-372 (2003).
126. S. M. Cheyne, in *Primate locomotion: linking field and laboratory research*, K. D'Août, E. E. Vereecke, Eds. (Springer New York, New York, NY, 2011), pp. 201-213.
127. C. Thiel, K. Kessler, A. Giessl, A. Dimmler, S. A. Shalev, S. von der Haar, M. Zenker, D. Zahnleiter, H. Stoss, E. Beinder, R. Abou Jamra, A. B. Ekici, N. Schroder-Kress, T. Aigner, T. Kirchner, A. Reis, J. H. Brandstatter, A. Rauch, *NEK1* mutations cause short-rib polydactyly syndrome type majewski. *Am J Hum Genet* **88**, 106-114 (2011).
128. J. El Hokayem, C. Huber, A. Couvé, J. Aziza, G. Baujat, R. Bouvier, D. P. Cavalcanti, F. A. Collins, M.-P. Cordier, A.-L. Delezoide, M. Gonzales, D. Johnson, M. Le Merrer, A. Levy-Mozziconacci, P. Loget, D. Martin-Coignard, J. Martinovic, G. R. Mortier, M.-J. Perez, J. Roume, G. Scarano, A. Munnich, V. Cormier-Daire, *NEK1* and *DYNC2H1* are both involved in short rib polydactyly Majewski type but not in Beemer Langer cases. *J Med Genet* **49**, 227-233 (2012).
129. J. M. Vazquez, V. J. Lynch, Pervasive duplication of tumor suppressors in Afrotherians during the evolution of large bodies and reduced cancer risk. *Elife* **10**, (2021).
130. J. G. M. Thewissen, L. N. Cooper, J. C. George, S. Bajpai, From land to water: the origin of whales, dolphins, and porpoises. *Evo Edu Outreach* **2**, 272-288 (2009).
131. W. L. Jungers, in *Size and scaling in primate biology*, W. L. Jungers, Ed. (Springer US, Boston, MA, 1985), pp. 345-381.
132. A. M. Rudolf, Q. Wu, L. Li, J. Wang, Y. Huang, J. Togo, C. Liechti, M. Li, C. Niu, Y. Nie, F. Wei, J. R. Speakman, A single nucleotide mutation in the dual-oxidase 2 (*DUOX2*) gene causes some of the panda's unique metabolic phenotypes. *Natl Sci Rev* **9**, nwab125 (2022).
133. K. R. Johnson, C. C. Marden, P. Ward-Bailey, L. H. Gagnon, R. T. Bronson, L. R. Donahue, Congenital hypothyroidism, dwarfism, and hearing impairment caused by a missense mutation in the mouse dual oxidase 2 gene, Duox2. *Mol Endocrinol* **21**, 1593-1602 (2007).
134. J. G. Fleagle, *Primate adaptation and evolution*. (Academic press, 2013).
135. K. Milton, Physiological ecology of howlers (*Alouatta*): energetic and digestive considerations and comparison with the Colobinae. *Int J Primatol* **19**, 513-548 (1998).
136. I. Matsuda, C. A. Chapman, M. Clauss, Colobine forestomach anatomy and diet. *J Morphol* **280**, 1608-1616 (2019).
137. M. C. Janiak, Digestive enzymes of human and nonhuman primates. *Evol Anthropol* **25**, 253-266 (2016).

138. J. J. Kim, R. Miura, Acyl-CoA dehydrogenases and acyl-CoA oxidases. Structural basis for mechanistic similarities and differences. *Eur J Biochem* **271**, 483-493 (2004).
139. C. Matziouridou, S. D. C. Rocha, O. A. Haabeth, K. Rudi, H. Carlsen, A. Kielland, iNOS- and NOX1-dependent ROS production maintains bacterial homeostasis in the ileum of mice. *Mucosal Immunol* **11**, 774-784 (2018).
140. C.-J. Li, R. W. Li, R. L. Baldwin Vi, Assembly and analysis of changes in transcriptomes of dairy cattle rumen epithelia during lactation and dry periods. *Agric Sci* **9**, 619-638 (2018).
141. M. C. Janiak, A. S. Burrell, J. D. Orkin, T. R. Disotell, Duplication and parallel evolution of the pancreatic ribonuclease gene (*RNASE1*) in folivorous non-colobine primates, the howler monkeys (*Alouatta spp.*). *Sci Rep* **9**, 20366 (2019).
142. P. Pontarotti, *Evolutionary biology-mechanisms and trends*. (Springer Science & Business Media, 2012).
143. N. J. Dominy, P. W. Lucas, Ecological importance of trichromatic vision to primates. *Nature* **410**, 363-366 (2001).
144. N. G. Caine, N. I. Mundy, Demonstration of a foraging advantage for trichromatic marmosets (*Callithrix geoffroyi*) dependent on food colour. *Proc Biol Sci* **267**, 439-444 (2000).
145. A. C. Smith, H. M. Buchanan-Smith, A. K. Surridge, D. Osorio, N. I. Mundy, The effect of colour vision status on the detection and selection of fruits by tamarins (*Saguinus spp.*). *J Exp Biol* **206**, 3159-3165 (2003).
146. S. Heritage, Modeling olfactory bulb evolution through primate phylogeny. *PLoS One* **9**, e113904 (2014).
147. A. Matsui, Y. Go, Y. Niimura, Degeneration of olfactory receptor gene repertories in primates: no direct link to full trichromatic vision. *Mol Biol Evol* **27**, 1192-1200 (2010).
148. T. D. Smith, K. P. Bhatnagar, Microsmatic primates: reconsidering how and when size matters. *Anat Rec B New Anat* **279**, 24-31 (2004).
149. A. Berghard, A. C. Hagglund, S. Bohm, L. Carlsson, *LHX2*-dependent specification of olfactory sensory neurons is required for successful integration of olfactory, vomeronasal, and GnRH neurons. *FASEB J* **26**, 3464-3472 (2012).
150. J. Hirota, P. Mombaerts, The LIM-homeodomain protein LHX2 is required for complete development of mouse olfactory sensory neurons. *Proc Natl Acad Sci U S A* **101**, 8751-8755 (2004).
151. H. Li, R. Durbin, Inference of human population history from individual whole-genome sequences. *Nature* **475**, 493-496 (2011).
152. A. D. Barnosky, P. L. Koch, R. S. Feranec, S. L. Wing, A. B. Shabel, Assessing the causes of late Pleistocene extinctions on the continents. *Science* **306**, 70-75 (2004).
153. X. Luo, Y. Liu, D. Dang, T. Hu, Y. Hou, X. Meng, F. Zhang, T. Li, C. Wang, M. Li, H. Wu, Q. Shen, Y. Hu, X. Zeng, X. He, L. Yan, S. Zhang, C. Li, B. Su, 3D Genome of macaque fetal brain reveals evolutionary innovations during primate corticogenesis. *Cell* **184**, 723-740.e721 (2021).

154. C. Yang, Y. Zhou, S. Marcus, G. Formenti, L. A. Bergeron, Z. Song, X. Bi, J. Bergman, M. M. C. Rousselle, C. Zhou, L. Zhou, Y. Deng, M. Fang, D. Xie, Y. Zhu, S. Tan, J. Mountcastle, B. Haase, J. Balacco, J. Wood, W. Chow, A. Rhie, M. Pippel, M. M. Fabiszak, S. Koren, O. Fedrigo, W. A. Freiwald, K. Howe, H. Yang, A. M. Phillippy, M. H. Schierup, E. D. Jarvis, G. Zhang, Evolutionary and biomedical insights from a marmoset diploid genome assembly. *Nature* **594**, 227-233 (2021).
155. G. Dumas, S. Malesys, T. Bourgeron, Systematic detection of brain protein-coding genes under positive selection during primate evolution and their roles in cognition. *Genome Res* **31**, 484-496 (2021).
156. J. K. Rilling, Human and nonhuman primate brains: are they allometrically scaled versions of the same design? *Evol Anthropol* **15**, 65-77 (2006).
157. H. Stephan, H. Frahm, G. Baron, New and revised data on volumes of brain structures in insectivores and primates. *Folia Primatol (Basel)* **35**, 1-29 (1981).

Acknowledgments

We are grateful to the many individuals in our host institutions who have provided support for this project.

Funding

This work was supported by the Strategic Priority Research Program of the Chinese Academy of Sciences (XDPB17, XDB31020000), the National Natural Science Foundation of China (31822048 and 32270500), Yunnan Fundamental Research Project (2019FI010), the Animal Branch of the Germplasm Bank of Wild Species of Chinese Academy of Science (the Large Research Infrastructure Funding), International Partnership Program of Chinese Academy of Sciences (No. 152453KYSB20170002). This work was also partially supported by a Villum Investigator Grant (No. 25900) to G.Z. T.M.B. was supported by funding from the European Research Council (ERC) under the European Union's Horizon 2020 research and innovation programme (grant agreement No. 864203), BFU2017-86471-P (MINECO/FEDER, UE) and Howard Hughes International Early Career.

Author contributions

D.D.W. and G.J.Z. led the project. D.D.W., G.J.Z., X.G.Q. conceived and designed the research. D.D.W., G.J.Z. and Y.S. wrote the manuscript. Y.S. drafted the manuscript. Y.S., L.Z, F.L., L.Z., B.L.Z., F.S., J.W.C., C.Y.C., X.P.B., X.L.Z., H.L.Z., I.R.G., S.W., Y.M.W., L.K., G.L., H.M.L., Y.L., and P.D.S. performed comparative genomics analysis. L.Z., J.H, Z.Y.S, X.L., D.P.W., and K.F. contributed genome sequencing, assembly and annotation. P.F.F., M.L., Z.J.L., G.P.T., A.D.Y., C.R., T.H., T.M.B., and J.R. collected samples. J.R. and T.M.B. generated some genome assemblies for our comparative genomics analysis. C.R., G.P.T., J.R., L.Y., M.H.S., D.N.C., Y.G.Y., Y.P.Z., W.W. and X.G.Q. provided comments for improving the manuscript. Y.S., X.G.Q., and L.Z. plotted and revised figures. D.N.C. polished the manuscript. All authors approved the final manuscript.

Competing interests

The authors declare no competing financial interest.

Data and materials availability

All 27 primate genome assemblies and the raw genome long- and short-read sequencing data were deposited at the National Center for Biotechnology Information (NCBI) Assembly Database (https://www.ncbi.nlm.nih.gov/assembly/) and the Sequence Read Archive Database (https://www.ncbi.nlm.nih.gov/sra/) under the accessible BioProject accession codes: PRJNA785018 and PRJNA911016. We have uploaded all genome annotation GFF files to the figshare database (DOI: https://doi.org/10.6084/m9.figshare.21692894.v1). The positively selected genes and their sequence alignments also were uploaded to the public Dryad dataset (DOI: https://doi.org/10.5061/dryad.8w9ghx3qj).

Supplementary Materials

Materials and Methods

Figs. S1 to S39

Tables S1 to S42

References (158-228)

Figure legends

Fig. 1. Genomic phylogeny of primates. The maximum likelihood method was used to infer the primate species tree from whole–genome sequences across 52 species including 50 primate species and two outgroup species (Sunda flying lemur and Chinese tree shrew) with 100 bootstraps under a GTR+GAMMA model. The divergence time was estimated using fossil calibrations (Fig. S11) and the MCMCtree algorithm. The red and blue species names represent those genomes newly produced in this study. The genomes of the species marked in blue were assembled at the chromosome level. The genomes of the species marked in black were downloaded from the NCBI and Ensembl databases (table S8). Monkey pictures are copyrighted by Stephen D. Nash/IUCN/SSC Primate Specialist Group, and are used in this study with their permission.

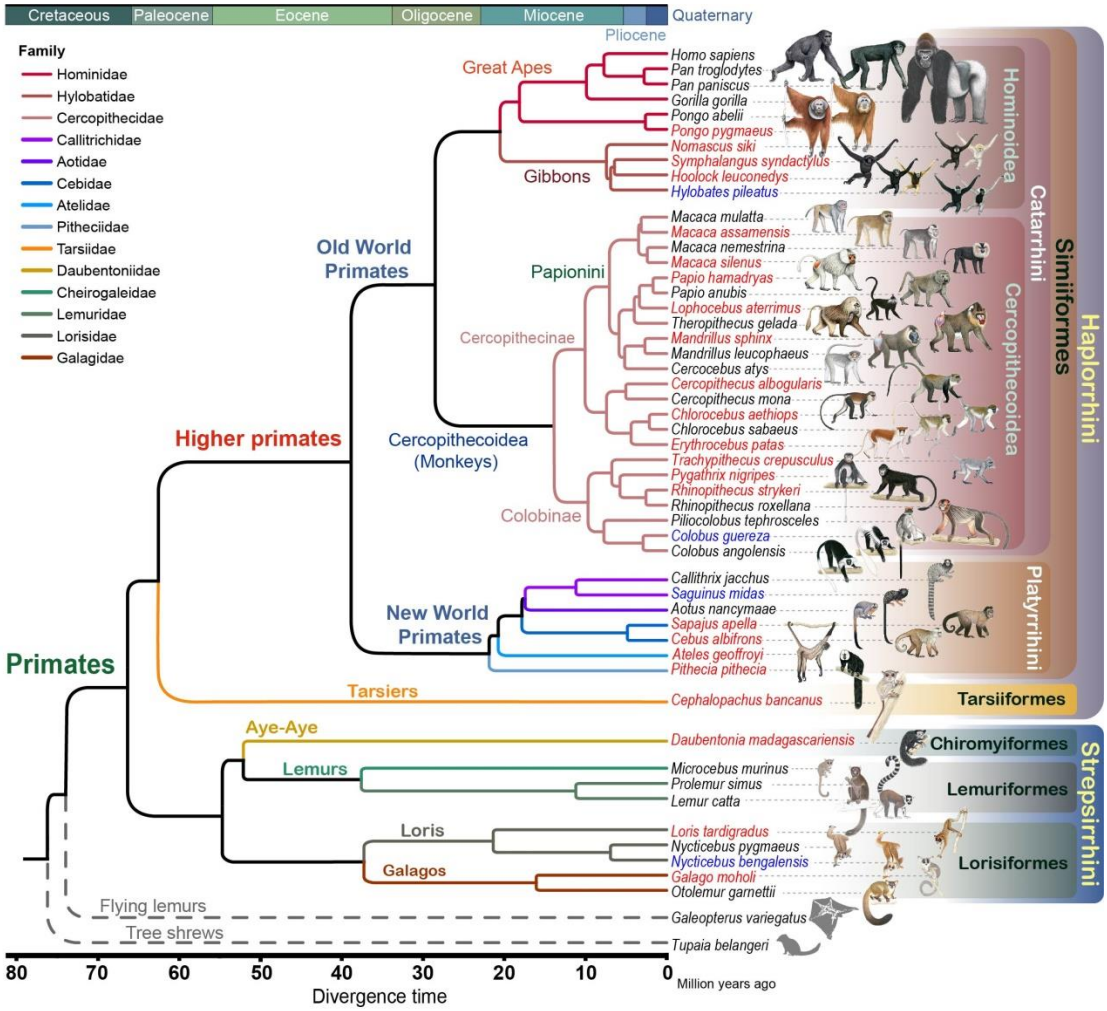

Fig. 2. Reconstruction of primate ancestral chromosomes. (A) Chromosome evolution patterns from the primate common ancestral lineage leading to the human lineage. Chromosomes are colored on the basis of human homologies. (B) Karyotype evolution and genome rearrangement. The rates of genomic rearrangement are highlighted in black bold font. Chromosome variations from ancestral nodes to derived branches are shown by pathways including chromosome reversal, translocation, fission and fusion events (shown in Fig. 2B by the number, e.g., reversal/translocation/fission/fusion). 'HYLPIL' represents the gibbon *Hylobates pileatus*, the genome of which was assembled at the chromosome level.

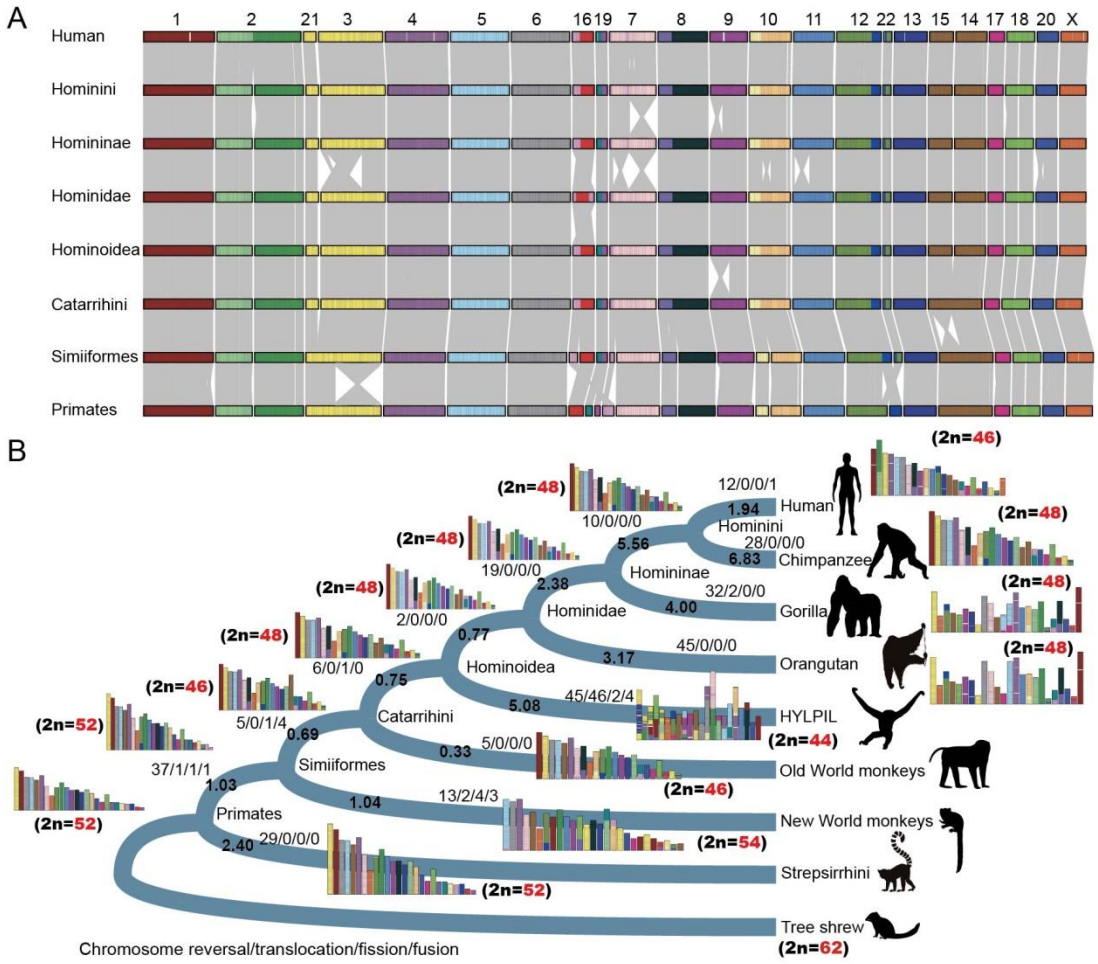

Fig. 3. Structural evolution in primate genomes. (A) Evolutionary pattern of lineage-specific segmental duplications in primates. The numbers of lineage-specific segmental duplications are given in red. The largest number of segmental duplications was found in the great ape lineage. OWMs: Old World monkeys. NWMs: New World monkeys. (B) An example of specific segmental duplications during evolution of the genome in Catarrhini. A gene pair overlapping the segmental duplication (*CCL4*, left; *CCL4L2*, right) is associated with HIV susceptibility. The red and green boxes represent the segmental duplication region and the overlapping gene pair, respectively. (C) The substitution rates across five evolutionary branches in primates. OWMs: Old World monkeys. NWMs: New World monkeys. (D) Evolutionary constraints of tissues across diverse lineages in primates. The evolutionary constraints of tissues are shown by the d_N/d_S median of tissue-specific expressed genes in different evolutionary nodes among primates.

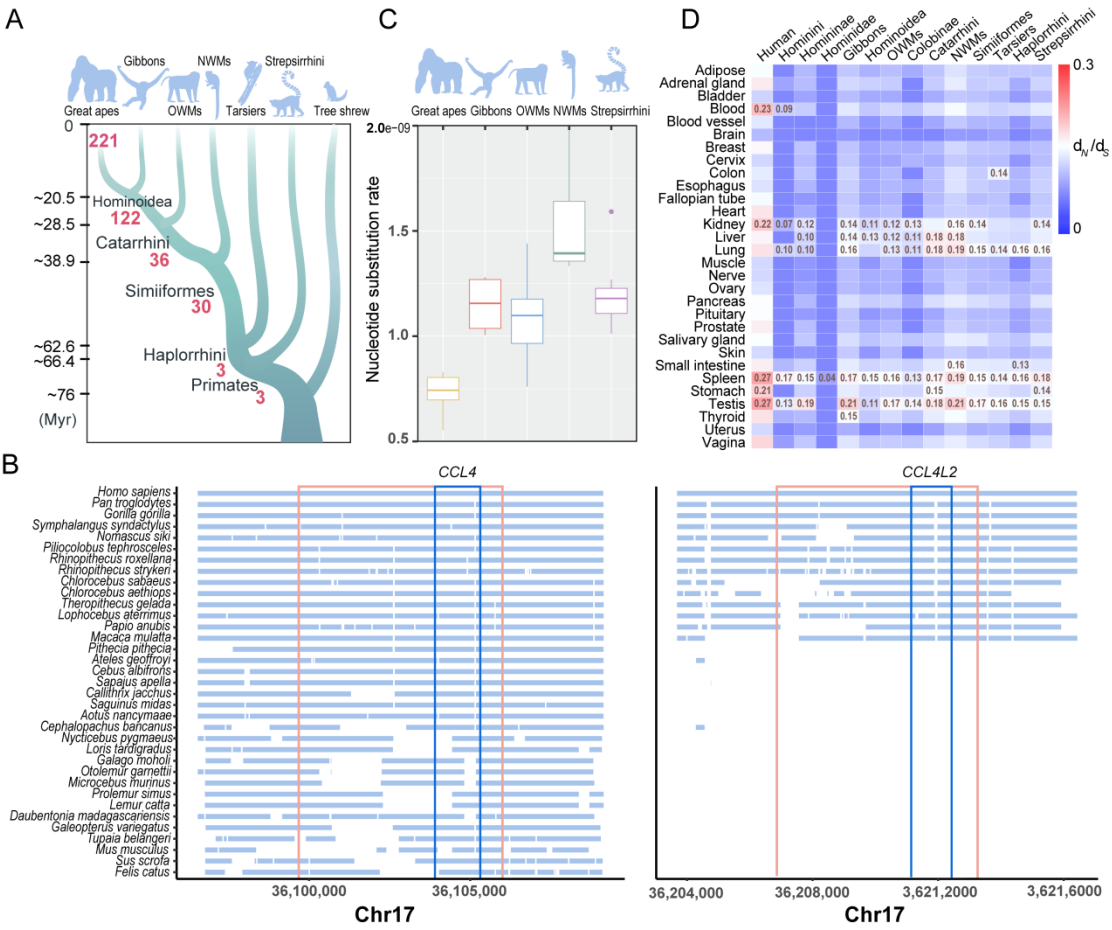

Fig. 4. Genomic changes and phenotype evolution in the ancestor of the Simiiformes. (A) An increased level of genomic evolutionary change including positively selected genes, lineage-specific accelerated regions, and significantly expanded gene families in the Simiiformes ancestral lineage. The brain sizes and brain structures are shown in representative evolutionary groups of primates. The brain sizes across primate and outgroup species derived from the previous studies (*156*, *157*). Brain images are from the Michigan State Comparative Mammalian Brain Collections (www.brainmuseum.org). (B) Representative phenotype variations including brain size and body mass between Simiiformes and Strepsirrhini/Tarsiiformes. Statistical significance (*P* value) was assessed by the Mann-Whitney *U* test with $P < 0.05$. (C) Candidate genes involved in the Axon guidance KEGG pathway (hsa04360). Genes relating to genomic changes in the Simiiformes ancestral lineage are shown in this pathway. The protein product of the positively selected gene (*SEMA3B*) in the Simiiformes ancestral lineage is coloured in red. The protein products of genes associated with lineage-specific accelerated regions (*EPHA3*, *RAC1*, *NTNG2* and *SEMA3D*) are marked in blue. (D) The Hippo signaling pathway (hsa04390) – involved in organ size and body size with candidates including positively selected genes and genes associated with lineage-specific accelerated regions. The gene products for positively selected genes (*LIMD1*, *BIRC3* and *STK3*) in the Simiiformes ancestral lineage are highlighted in red, whereas the products of genes associated with lineage-specific accelerated regions (*PATJ*, *SOX2*, *BMP2*, *DLG2* and *YWHAQ*) in the Simiiformes ancestral lineage are marked by blue. (E) Multiple sequence alignments of two positively selected genes, *TAS1R1* and *KIT*, along the Simiiformes ancestral lineage. The phylogenetic position of the Simiiformes ancestor is shown by a red arrow.

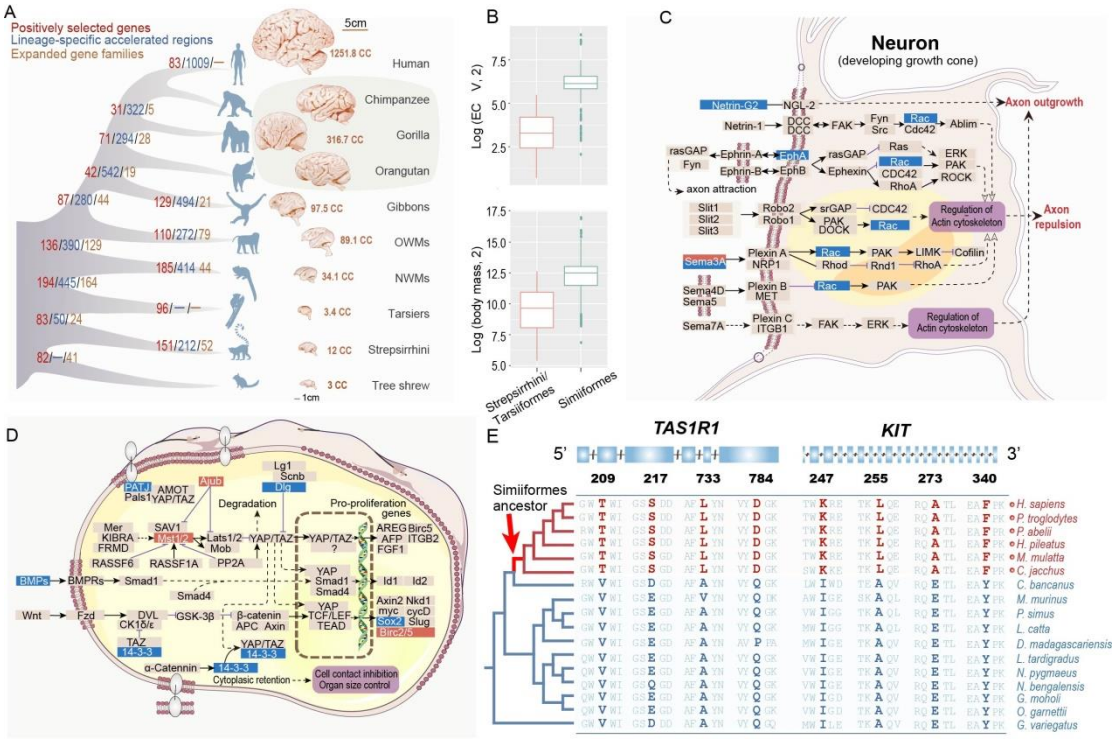

Fig. 5. Associations between genomic evolutionary characteristics and phenotypic traits in primates. (A) Positively selected genes and genes associated with lineage-specific accelerated regions, from the primate ancestral lineage leading to the human lineage, involved in transport, release and receptors in neurotransmitter signaling. (B) *NEK1* gene involved in upper limb bone development was under positive selection with three positively selected sites in the gibbon ancestral lineage. The gibbon ancestor is marked in red. (C) Eight positively selected genes/genes associated with lineage-specific accelerated regions from the great ape ancestral lineage involved in the TGF-β, Wnt and Hippo signaling pathways. (D) Positively selected genes and genes associated with lineage-specific accelerated regions involved in the evolution of the digestive system in the Colobinae ancestral lineage. Genes marked in red and blue represent positively selected genes and genes associated with lineage-specific accelerated regions, respectively, in this lineage.

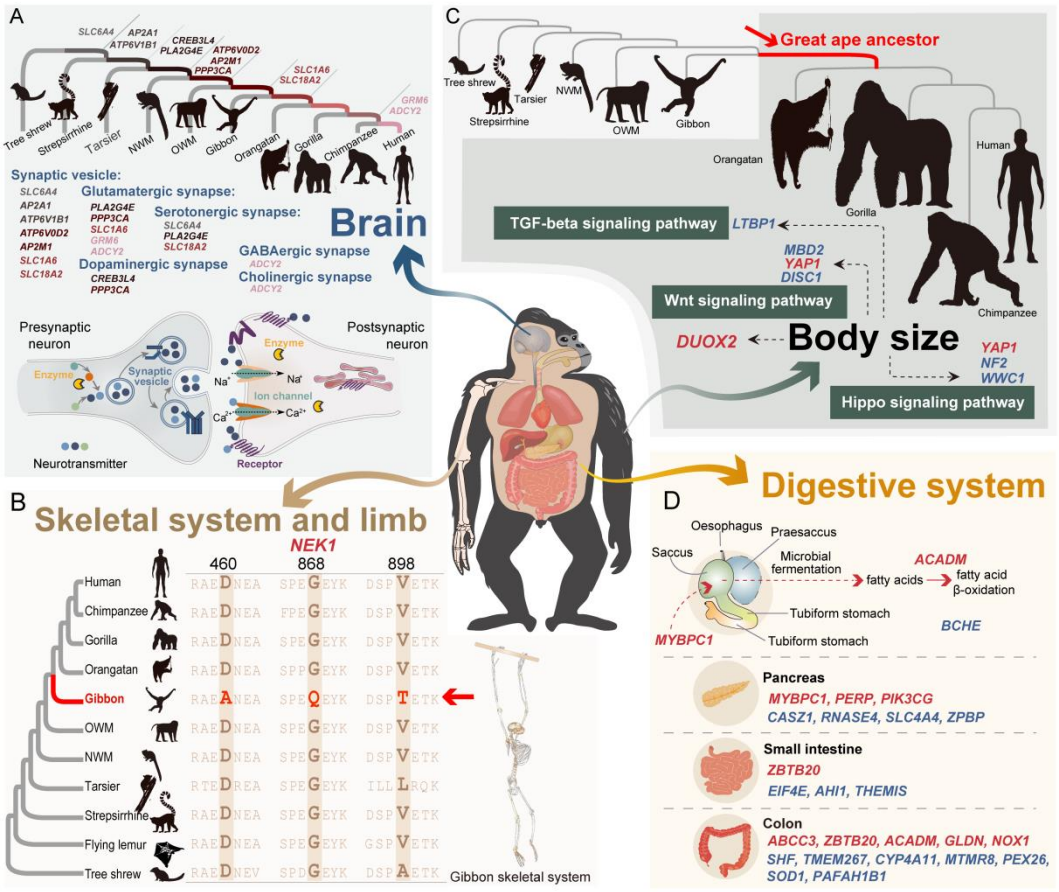

Fig. 6. Demographic history of non-human primates. (A) Primate species were grouped according to their biogeographic distribution (Africa, Asia and South America). The plot shows the normalized demographic history of all species within each biogeographic region. The normalized *Ne* was inferred by dividing the estimated value of *Ne* for each species at each time point by its maximum value. *Callithrix jacchus* was removed from this analysis because the genome was derived from an inbred individual. The time period from 50,000 to 20,000 years ago (late Pleistocene) is highlighted by a grey background. (B) Correlation analysis between nucleotide diversity and *Ne* after phylogenetic correction using the Ape library in R (http://ape-package.ird.fr/). *Ne* represents the median value of effective population size for each species 20,000 years ago. (C) Nearly half (n=20) of all non-human primate species experienced a continual decline in *Ne* over the past 3 million years (My). These include 13 critically endangered or endangered species highlighted in red. The IUCN Red List status was marked for each species in the inserted plot. CR= Critically Endangered; EN=Endangered, VU= Vulnerable; NT=Near threatened; LC=Least concern.